Effect of NFE2L1 Overexpression and Knock Down on the Response of XBP1 Splice Variants to Endoplasmic Reticulum Stress

By

Jacob Billingsley

B.Sc., Carleton University, 2018

A thesis submitted to the Faculty of Graduate Studies and Postdoctoral Affairs in partial fulfillment of the requirements for the degree of Master of Biology with a specialization in Biochemistry

Carleton University

Ottawa, Ontario, Canada

January 2021

Abstract

The unfolded protein response (UPR) is responsible for the degradation and refolding of misfolded proteins. Nuclear factor erythroid-2 like-1 (NFE2L1) basic leucine zipper (bZIP) transcription factor which respond primarily to oxidative stress and proteasome inhibition. In its role in maintaining proteostasis, NFE2L1 upregulates production of proteasomal subunits. Over the years, functional similarities and parallel response pathways have been observed between the UPR and NFE2L1. NFE2L1 may be involved in maintaining proteostasis via involvement in the UPR, directly. The activation of XBP1, a UPR effector, was analyzed under NFE2L1 knock down and overexpression. At the protein level, NFE2L1 knock down decreases the amount of activated XBP1 produced when treated with thapsigargin. NFE2L1 overexpression increased activated XBP1 synthesis under untreated conditions. NFE2L1 knock down resulted in significantly disrupted splicing of XBP1 RNA into its active form. These results suggest that NFE2L1 expression has an impact on UPR signaling.

Acknowledgements

I would first like to thank all educators at Carleton for providing a safe and nurturing environment for its students to learn and grow. In particular, I would like to thank those who saw potential in me when I perhaps did not see it in myself. Taking a chance on a student with a mixed academic record is a risk that Carleton educators were willing to take on me. Drs. Jefferey Dawson, Iain McKinnell and Bill Willmore all took that chance with me and I am extremely grateful. Dr. Willmore has worked exceptionally hard to teach me all the techniques I currently routinely apply in the lab; he stayed late nights, came in on weekends, and has even appeared late to important meetings because of his dedication to my development. Beyond lab work, I have always known that I can go to Dr. Willmore if ever I feel anxious about my work or my future in the field; I consider myself extremely lucky to have found such a supportive supervisor and will remember these sacrifices if a time should come that I am in his position. I also thank the members of my lab and those of the Biggar lab for their friendship, thoughtful suggestions, and advice; these include Shana, Jessica, Rowida, both Matthews, Anand, Ryan, Hemanta and Valentina. In particular, I thank Rowida for being my strongest supporter throughout and essential in times when I doubted myself.

Beyond my lab, I must thank Sabrina Dawson and Claudia Buttera in both their roles as educators and as supervisors in my work as a teaching assistant. They have shown me in their own ways what it means to stand strong, be kind, and lead.

I am also extremely thankful to those who have taken time out of their busy schedule to stand on my graduate advisory committee and offer their advice to further assist in my professional development. Thank you, Drs. Carolina Ilkow, Bruce McKay, and again, Bill Willmore

I would not be where I am today without the continued love and support of my friends and family, who have always been there to encourage me every step of the way. I am eternally grateful that I am fortunate enough to be able to pursue my passion, and for this I thank my father Perry and my stepmother Deb for their continued support of my ambitions. I must also thank Abbey for being the most amazing partner throughout the toughest years of my undergraduate and master's degrees.

I dedicate my thesis to my late mother Justine. As I grow and develop, I may on occasion lose sight of what is most important, but I will always find my way when I remember in your memory what I must continue to fight for.

Table of Contents

List of Figures

List of Tables

List of Abbreviations

ARE	Antioxidant Response Element
ATF 4/6	Activating Transcription Factor 4 (or 6)
bZIP	Basic Leucine Zipper
Bip	Binding immunoglobulin protein
Ca^{2+}	Calcium
Cdc48	Cell-division cycle-48
C/EBP	CCAAT/Enhancer-Binding Protein
CHOP	C/EBP-Homologous Protein
CNC	Cap n' Collar
CNX	Calnexin
CRT	Calreticulin
DNA	Deoxiribo Nucleic Acid
DMSO	Dimethylsulphoxide
EDEM	ER degradation-enhancing alpha-mannosidase protein
eIF2α	Eukaryotic Initiating Factor 2 alpha
ER	Endoplasmic Reticulum
ERAD	ER-Associated Degradation
FBS	Fetal bovine serum
GADD34	Growth Arrest and DNA Damage-Inducible (protein) 34
GPT	N-acetylglucosaminephosphotransferase
GPX1	Glutathione peroxidase
GRP78	Glucose Regulated Protein 78
GST	Glutathione S-transferase
Herpud1	endoplasmic reticulum stress-inducible, ubiquitin-like domain member 1
HSP	Heat shock proteins
IP3	1,4,5-trisphosphate
IRE1α	Inositol-Requiring Enzyme 1 alpha
MAM	Mitochondrial-associated ER membrane
mRNA	Messenger Ribonucleic Acid
NFE2L1/2/3	Nuclear Factor Erythroid 2-Like-(1/2/3)
NGLY1	N-glycanase 1
OST	Oligosaccharyltransferase
PERK	PKR-Like ER Kinase
PDI	Protein Disulphide Isomerase
PVDF	Polyvinylidene difluoride
RIPA	Radioimmunoprecipitation assay
RNA	Ribonucleix Acid
ROS	Reactive oxygen species
RT-qPCR	Real Time Quantitative Polymerase Chain Reaction
RyR	Ryanodine receptors

SEL1L	Sel-1 homolog 1
SEM	Standard error of the mean
SENP1	SUMO specific protease 1-mediated
SERCA	Sarcoendoplasmic reticulum calcium ATPase
SREBP1	Sterol-regulatory element binding protein family of transcription factors
SRP	Signal recognition particle
TCE	Trichloroethanol
Th	Thapsigargin
TPR	Tetratricopeptide
UGGT1 and UGGT2	UDP-glucose:glycoprotein–glucosyltransferases
UPR	Unfolded Protein Response
XBP1	X-Box Binding Protein 1
XBP1(S)	XBP1 (Spliced)
XBP1(U)	XBP1 (Unspliced)

Chapter 1. Introduction

1.1 The Endoplasmic Reticulum

The endoplasmic reticulum (ER) is an often-overlooked organelle governing various essential cellular processes autonomously, as well as being critical in organellar crosstalk. The ER is primarily known for its protein processing capabilities; one third of the proteome is partially processed in this organelle, many destined for secretion or membrane integration (McCaffrey & Braakmen, 2016). The ER lumen is a very distinct microenvironment within the cell, when compared to the cytosol. Particular types of posttranslational modifications can only take place within this controlled, unique environment (Sevier & Kaiser, 2008). To access this environment, a nascent polypeptide requires a N-terminal hydrophobic signal to bind a signal recognition particle (SRP) in the cytosol (the KDEL sequence targets the protein to the ER membrane). This SRP must have the ability to pause translation of the nascent polypeptide until such a time as the SRP is bound to a receptor on the ER membrane, and the hydrophobic N-terminus of the peptide is docked within a transmembrane translocon (Lakkaraju *et al*., 2008). Translation then resumes and the protein is injected directly into the ER lumen, after which the hydrophobic signal is cleaved, the SRP and the ribosome dissociate from the translocon, and the protein is further processed in the ER lumen. Glycosylation of secreted and membrane-bound proteins occurs simultaneously as translation and transition through the ER translocon. Highlighting the importance of protein processing in the ER is how this process of ER targeting and translocation is conserved in all eukaryotes (Strub *et al*., 1991)

Once nascent polypeptides enter the ER, protein folding begins immediately; chaperone proteins crowd the luminal translocon and surround the nascent polypeptide as it enters;

modifications to the protein occur at such a rate that the chaperones are limited only by the speed of translation (Braakman & Bulleid, 2011). Among the modifications performed in the ER lumen are hydroxylation, proteolytic cleavages, and protein folding, in addition to those that are unique to the luminal environment such as disulphide bond formation and asparagine-linked glycosylation (McCaffrey & Braakman, 2016). Accompanying the proteins effecting these modifications are those that facilitate their catalytic activity, responsible for ATP hydrolysis of ATP-bound chaperones, and those catalyzing the release of ATP. Further, chaperones may play roles in essential and non-obvious protein folding tasks such as stabilizing intermediates and inhibiting the aggregation of incompletely-folded proteins (McCaffrey & Braakman, 2016).

Secreted and membrane-bound proteins, in general, are synthesized and folded at the ER. Protein folding in the ER involves two different pathways; one pathway for non-glycosylated proteins and the other pathway for glycosylated proteins (Ellgaard *et al*., 2016). Chaperone proteins collectively make up the "chaperome" and distinct chaperone proteins are associated with ribosomes at each cellular compartment. Families of chaperone proteins include the heat shock proteins (HSP): HSP90s, HSP70s, HSP60s, HSP40s, prefoldins, small HSPs (sHSPs), tetratricopeptide repeat (TPR)-domain-containing proteins, and organellar-specific chaperones of the ER and mitochondria (reviewed by Brehme *et al*., 2019). At the ER, these include glucose-regulated protein-78 (GRP78 or heat shock protein 70 kDa protein 5 (HSPA5); also known as Binding immunoglobulin Protein (BiP)) (reviewed by Pobre *et al*., 2019; Wang *et al*., 2017; Ibrahim *et al*., 2019.), serpin H1 (HSP47), GRP94 (gp96 or HSP90B1), GRP170 (ORP150 or HYOU1), calnexin (CNX; IP90, major histocompatibility complex class I antigen-binding protein p88, or p90), calreticulin (CRT or CALR) and P4HB (PDIA1), a member of the protein disulfide isomerase (PDI) family (Graner *et al*., 2015). These chaperones can associate with either non-

glycosylated or N-linked-glycosylated proteins made at the ER and are responsible for their proper folding and disulfide bond formation.

1.1.1 Protein quality control in the ER

Once a polypeptide enters the ER and is folded by molecular chaperones in the lumen, proteins are subject to protein quality control. Unchecked, the misfolding of proteins can be extremely deleterious to cellular function, and misfolded proteins secreted from the cell in exosomes could spread this disfunction to organ systems. Thus, a final check for protein folding quality control is performed, and a complex system of proteins is responsible for refolding or degrading these misfolded proteins (Phillips *et al*., 2020). The recognition of misfolded proteins is a very complex network of chaperones which have affinity for structural irregularities associated with misfolding. In some cases, there are chaperone proteins produced solely to recognize incorrect products of other closely related chaperone proteins, and target the misfolded product for proteasomal-mediated degradation (Sun & Brodsky, 2019). Further, in the relatively complicated SRP system discussed previously, mistakes regarding cellular localization sometimes occur. The result is an incomplete protein free in the cytosol. Though the cytotoxic aggregation of such proteins is always of concern in the cell, proteins containing hydrophobic domains are particularly prone to aggregation because of the aqueous nature of the cytosol. To combat this, there are proteins with hydrophobic sequence recognition sites which irreversibly bind these hydrophobic domains, preventing aggregation, and possess signal sequences for ubiquitination and degradation. (Guna & Hegde, 2018). If misfolded proteins cannot be degraded conventionally, such as in the case of irreversible hydrophobic interactions shielding a

conventional chaperone-binding site, such proteins can be targeted for autophagy and degraded by fusion with a lysosome (Sun & Brodsky, 2019).

1.1.2 ER Homeostasis

To perform these functions, the ER environment is very tightly regulated and is distinct from the cytosol in many ways. Primarily, the ER serves as a major calcium (Ca^{2+}) store in the cell (Verkhratsky & Toescu, 2003). As it relates to protein folding, calcium is an important cofactor necessary for the proper functioning of many chaperone proteins. Calcium depletion is highly detrimental to the ER lumen and results in the accumulation of misfolded and unfolded proteins (Gidalevitz *et al*., 2013; Bian *et al*., 2016). The primary methods by which calcium enters the ER is through the P-type transmembrane pump termed the sarcoendoplasmic reticulum calcium ATPase (SERCA). SERCA pumps calcium from the cytosol into the ER lumen, as well from another major calcium store, the mitochondrial associated ER membrane (MAM) microenvironment (Gidalevitz *et al*., 2013; Bian *et al*., 2016). Calcium is released from the ER through the intracellular second messenger 1,4,5-trisphosphate (IP3) and ryanodine receptors (IP3Rs, RyRs). These play an important role in calcium signaling to the mitochondria as part of apoptotic signaling (Crompton *et al*., 1987).

In addition to carefully regulating ER luminal calcium, the ER must also regulate the redox potential as a facilitating environment in the formation of new bonds between amino acids and moieties. For PDIs to efficiently effect protein folding by the formation of disulphide bonds, the ER must maintain a favourable redox environment for the oxidation of cysteines in the chaperone binding pocket (Sevier & Kaiser, 2008). Ero1 is the oxidoreductase primarily responsible for the activation of PDI proteins by reoxidation such that they can subsequently

oxidize cysteine residues on their target proteins. However, Ero1 activity is a source of hydrogen peroxide in the ER. This is because Ero1 oxidizes PDIs proteins while simultaneously reducing oxygen, producing one molecule of hydrogen peroxide (Tavender & Bulleid, 2010). Several ER oxidoreductases are produced to reduce this stressor (Zhang *et al*., 2019). Regulatory cysteines on Ero1 modulate its activity and thus the activity of PDIs and the flow of oxidizing agents. If the ER environment becomes excessively oxidizing due to the accumulation of reactive oxygen species (ROS), the Ero1 regulatory cysteines are disulphide bonded, stabilizing its inactive state, reducing its ability to activate PDIs. In this way, the mechanism acts as a negative feedback loop; unrestrained oxidation of thiol groups generates ROS, which deactivates Ero1, inhibiting the activation of proteins responsible for the oxidation of thiol groups. Conversely, the accumulation of free thiols in the ER triggers the reduction of the bonded Ero1 regulatory cysteines, reinstating its capacity for activating PDIs, which then catalyze the formation of disulphide bonds. Thus, perturbations to the ER redox environment hold important implications regarding the cell's ability to perform protein folding; if ROS build up in the ER lumen, Ero1 would be negatively regulated, inhibiting the formation of disulphide bridges, a crucial post-translational modification (Sevier *et al*., 2007).

The lectin-like chaperones, CNX and CRT, are dependent on the presence of both monoglucosylated N-linked glycans and unfolded regions on nascent glycoproteins (reviewed extensively by Ellgard & Helenius, 2001; Ellgard & Helenius, 2003; Schrag *et al*., 2003). Both proteins bind to calcium and are part of the calreticulin/calnexin cycle which maintains protein quality control in the ER (Caramelo & Parodi, 2008). CNX is a type 1 ER transmembrane protein, and CRT a soluble, ER luminal protein. As proteins are synthesized at the ER, they enter

the ER lumen and are N-glycosylated by oligosaccharyltransferase (OST) as they emerge from the translocon. Two glucoses are removed by the sequential action of glucosidase I and II respectively to generate monoglucosylated species that are recognized by CNX and/or CRT. CNX binds N-glycoproteins that have Glc-NAc2-Man9-Glc1 oligosaccharides attached and associates with the protein disulfide isomerase ER protein 57 (also known as ER-60, GRP58 or ERp57). ERp57 is a ubiquitous ER thiol-dependent oxidoreductase that promotes the formation of intra- or intermolecular disulfide bonds during glycoprotein folding (Uhrigshardt *et* al., 2010; Marcus *et al*., 1996; High *et al*., 2000; Ellgard *et al*., 2003; Kostova & Wold, 2003; Määttänen *et* al., 2010). The CNX/CRT/ERp57 complex maintain glycosylated proteins in an unfolded state until the terminal glucose moiety is cleaved by glucosidase II (for an excellent review, see Määttänen *et* al., 2010). The folded state of the protein is then assessed by UDP-glucose:glycoprotein–glucosyltransferases-1 and -2 (UGGT1 and UGGT2) that adds a glucose moiety if the protein is incompletely folded, sending it back for more folding attempts (Määttänen *et* al., 2010). CRT binds to misfolded proteins and prevents their export from the ER to the Golgi complex (Shan *et al*., 2007). These chaperones are critical for various functions of the ER, including the sensing unfolded proteins, the binding of calcium and the sensing of cellular stress (including the UPR, oxidative stress, heat shock and the integrated stress response) (Brehme *et al*., 2019). CNX may act in assisting protein assembly and/or in the retention within the ER of unassembled protein subunits. Further, CNX and CRT buffer calcium in the ER lumen via several calcium-binding domains on each protein. CRT regulates the activity of SERCA 2b, providing dynamic control of ER calcium homeostasis (Nakamura *et* al., 2001; Li & Camacho, 2004). CNX is palmitoylated at cysteines 503 and 504 by the ER-resident palmitoyltransferase DHHC6, and the resulting structural reconfiguration allows the chaperone to interact with

SERCA. This interaction has been shown to modulate calcium homeostasis in the ER and the efficiency of calcium signaling to the mitochondria. CRT interacts with the luminal carboxy-terminal sequence of SERCA2b to inhibit calcium oscillations (Li & Camacho, 2004). Under conditions of cell stress, CNX becomes de-palmitoylated and interacts with ERp57 in order to execute its role in protein quality control (Lynes *et al*., 2013).

1.1.3 ER Environment Perturbation and Stress

Perturbations of ER homeostasis can alter the organelle's regulated environment and have a negative effect on protein folding. As described above, oxidative stress can have a negative impact on protein folding not only though the alteration of chaperone binding sites on proteins, but also in disrupting the activation of Ero1 (and subsequently PDIs) and disulphide bridge formation (Sevier *et al*., 2007). The disruption of calcium homeostasis can also impede the protein folding capabilities of chaperones for which it a necessary cofactor, such as CNX AND CRT (Caramelo & Parodi, 2008). These lead to the accumulation of misfolded or unfolded proteins in the ER. The exposed hydrophobic regions of these unfolded proteins may align with one another, leading to their aggregation. Additionally, proteins containing hydrophilic domains are particularly prone to such aggregations (Rousseau *et al*., 2006) The proteotoxicity resulting from such aggregates is termed ER stress, which is resolved through a process termed the unfolded protein response (UPR), discussed below. Many stressors can cause ER stress, such as hypoxia, oxidative stress, nutrient deficiency, calcium depletion, acidosis, and more (Moenner *et al*.,2007). To study ER stress, chemical treatments have been developed to specifically alter the ER lumen environment. These are more specific to the ER, rather than observing a general

response to a universal stressor such as oxidative stress, which initiates signaling cascades in all organelles. Though such treatments may still elicit a general toxic response, they are mechanistically intended for ER disruption. One such treatment is thapsigargin. Thapsigargin is a sesquiterpene lactone from the umbelliferous plant. Within the ER system, thapsigargin is a non-competitive inhibitor of SERCA. It binds SERCA at its calcium binding site, thus inhibiting the flow of calcium into the ER (Bian *et al*., 2016). The lumen is quickly compromised, calcium-dependent chaperone proteins become unable to effect protein folding without the required cofactor, thus resulting the accumulation of unfolded proteins (Hetz, 2012). Treating cells with thapsigargin to cause ER stress and elicit the UPR is well established in the literature, and a commonly practiced technique. Another staple treatment in the study of UPR is tunicamycin. Tunicamycin is a high-affinity inhibitor of N-acetylglucosaminephosphotransferase (GPT), and in doing so, inhibits asparagine glycosylation in the ER (Yoo *et al*., 2018). N-linked glycosylation is an important post-translational modification that may alter the solubility of proteins (Adams *et al*., 2019). As such, the inhibition of GPT results in the accumulation of hydrophobic domains of unfolded proteins, which are especially prone to aggregation (Yoo *et* al., 2018; Rousseau *et al*., 2006; Hetz, 2012).

1.2 Unfolded Protein Response

Dysregulation of the ER environment and the resulting perturbation of proteostasis are resolved by the UPR. Further, many reviews of the UPR, and the proteins involved, document the process of "sensing" unfolded proteins in the ER (High *et al*., 2000; Ellgard *et al*., 2003; Kostova & Wold, 2003). Briefly, during non-stress conditions, BiP binds to the luminal domains of three transmembrane stress sensing proteins a) inositol requiring enzyme 1α/β (IRE1α and IRE1β), b)

activating transcription factor 6α/β (ATF6a and ATF6b) and c) PKR-like ER kinase (PERK), keeping them in an inactive form. During ER stress, the association of misfolded proteins with BiP causes it to dissociate from the luminal domains of these proteins, leading to the activation of IRE1, ATF6 and PERK (Figure 1A).

Activation of ATF6 involves its dissociation from the ER membrane, transport from the ER to the Golgi, and its association with the Golgi-resident serine proteases SP1 and SP2 at the Golgi complex. SP1 and SP2 cleave off the N-terminus of ATF6 to produce ATF6-N, the active transcription factor domain of this protein (Määttänen *et al*., 2010). ATF6-N then travels to the nucleus, where it heterodimerizes with XBP1-s and activates the genes involved in the production of ER chaperones (including BiP and PDI), factors involved in ER biogenesis, lipid synthesis and factors involved in ER-associated degradation (ERAD; see below). Activation of PERK causes the cytosolic kinase domain of this protein to autophosphorylate, which in turn, phosphorylates eukaryotic initiation factor 2α (eIF2α). This initiates a cascade of gene expression which leads to the ultimate production of CCAAT/enhancer-binding protein (C/EBP)-homologous protein (CHOP), growth arrest and DNA damage–inducible 34 (GADD34) and ATF4. These, in turn, activate the expression of genes involved in the antioxidant response, amino-acid synthesis, and the apoptotic response. GADD34 controls the expression of proteins which act to dephosphorylate and restore proper function of eIF2α in an antagonistic manner to the function of PERK (Brehme *et* al., 2019) Activation of PERK halts the cell cycle and prevents further protein translation, preventing more proteins from entering the ER. Activation of IRE1 causes its autophosphorylation, dimerization and oligomerization into an active nuclease. This activated nuclease splices nascent XBP1 mRNA into its spliced variant (XBP1(S)) by removing a 26-nucleotide intron, triggering a translational frameshift. The product of translation of XBP1(S) mRNA is a 40kDa bZIP

transcription factor that binds to DNA directly or in association with the final product of ATF6 (Figure 1B). Transactivation activity of XBP1(S) protein is controlled by SUMO specific protease 1-mediated (SENP1) SUMOylation of two lysine residues in its DNA-binding domain (He *et ali*, 2010). The stability of XBP1(S) is enhanced by acetylation by p300, enhancing its transcriptional activity (Wang & Ouyang, 2010). Like other UPR effectors, XBP1 strongly enhances the production of chaperone proteins, but XBP1(S) specifically is crucial in the ERAD function of the UPR (Hetz, 2012).

The activation of BiP also ultimately triggers ERAD through which unfolded proteins are translocated from the ER lumen to the cytosol for subsequent ubiquitylation and degradation by the 26S proteasome (Missiroli *et* al., 2017; Kostova & Wolf, 2003). ERAD occurs in a series of steps which involves 1) recognition of unfolded/misfolded proteins by cytoplasmic and luminal chaperones and associated factors (Myhill *et al*., 2008), such as 70 kDa heat-shock protein (Hsp70)-family members, CNX and CRT, and PDIs, 2) the targeting of unfolded proteins for retrotranslocation (the retrotranslocon), 3) initiation of retrotranslocation of unfolded proteins from the ER lumen to the cytosol, 4) ubiquitination of the target protein by E3 ubiquitin ligases and glycosylation by the attachment of N-linked glycans and 5) degradation by the proteasome (reviewed by Lakkaraju *et al*., 2012). Initiation of retrotranslocation may require cell-division cycle-48 (Cdc48) complex, as well as other components, which glycosylate and polyubiquitinate the proteins targeted for degradation. The energy derived from ATP hydrolysis by Cdc48, which is a AAA+ATPase, is coupled to retrotranslocation. There are three checkpoints for proper protein folding within the ERAD; 1) the monitoring of the folded state of the cytosolic domains (often termed ERAD-C), 2) the monitoring of the folded state of the luminal domains (often termed ERAD-L) and 3) the monitoring of the transmembrane domains (often termed ERAD-M) of the of

the ER-membrane bound protein. Proteins must pass all three checkpoints to determine whether they require continuing through the ERAD process. ERAD is augmented by ER-derived autophagy, often called ERAD II, to remove aggregates too large to be dislocated across the ER membrane and targets them for lysosome-mediated degradation. Under severe or chronic stress, the UPR switches to an apoptotic response by the cell.

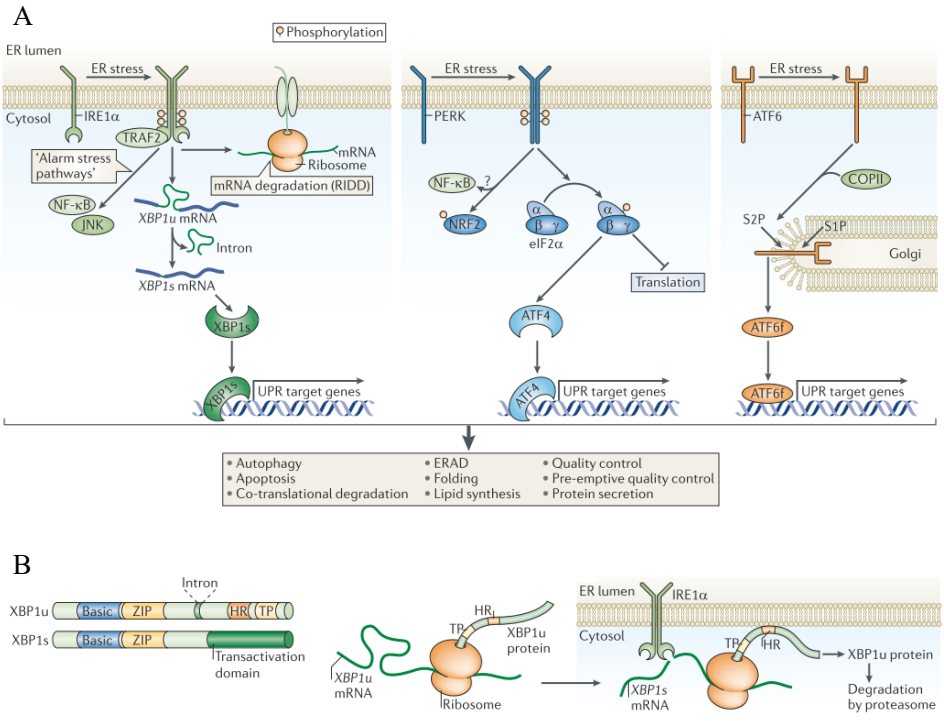

Figure 1: The three branches of the UPR (A), and the splicing of XBP1 (B). XBP1(U) protein possesses a translational pausing (TP) domain to halt its synthesis as the XBP1(U) mRNA-ribosome-nascent XBP1(U) protein complex is being translocated to the ER membrane via its hydrophobic region (HR). Figure from Hetz, 2012.

1.3 NFE2L1

Nuclear Factor Erythroid 2-like-1 (NFE2L1 or Nrf1) is a "cap and collar" (CNC) family bZIP transcription factor with relatively ubiquitous expression across tissue types. The CNC domain is a sequence of 43 amino acids that are highly conserved in metazoans, first identified in *Caenorhabditis* elegans and *Drosophila* (Sykiotis & Bohman, 2010). There are six CNC proteins in humans: NFE2L1, NFE2L2, NFE2L3, Bach 1, Bach 2 and p45/NFE2.

The most extensively studied of the three is NFE2L2, which is highly constitutively expressed across tissue systems (Robledinos-Anton *et al*., 2019). Its roles in responding to oxidative stress have been well-document, often considered the key regulator of the antioxidant response (Dobson *et al*., 2018). Oxidative stress is a staple of innumerable disease conditions, and thus expression of NFE2L2 is considered protective against neurodegeneration, cancer, diabetes, and many more (Sykiotis & Bohman, 2010; Gonzalez-Donquiles, 2017). Similarly, decreasing expression with aging has been suggested to be a contributing factor to deteriorating health in aging (Schmidlin *et al*., 2019).

With the exclusion of NFE2L2, NFE2L1 is the next best characterized of the CNC bZIP transcription factors. Unlike NFE2L2, in its inactive state, the full-length NFE2L1 is anchored to the ER membrane by a short, N-terminal amphipathic alpha helical domain. There are many isoforms of NFE2L1 as a result of alternative splicing and alternative start and stop codons (Kim *et al*., 2016). The longest isoform of is termed TCF11, which is the isoform that is bound to the ER membrane. In its inactive form, the NST domain of TCF11 is heavily glycosylated in the ER lumen. Upon activation by disruption of proteasome-mediated degradation or oxidative stress, the luminal-facing glycosylated NST domain TCF11 is retrotranslocated such that it faces the

cytosol. Essential to its activation is the subsequent deglycosylation of the NST domain, mediated by N-glycanase 1 (NGLY1). This is followed by the cleavage of its ER-membrane-bound domain, mediated by DDI-1/2 (Koizumi *et al*., 2016; Tomlin *et al*., 2017; Kim *et al*., 2016). This yields the active 95kDa transcription factor isoform of NFE2L1. Upon entering the nucleus, activated NFE2L1 heterodimerizes with small Maf proteins, enabling it to bind the antioxidant response element (ARE). The ARE is responsible for the transcription of proteins responsible for the reduction of ROS and the synthesis of the major cellular antioxidant glutathione (extensively reviewed in Kim et al., 2016). NFE2L2 and NFE2L1 overlap in function as it relates to antioxidant response, but are nonetheless both important in protecting the cell from oxidative stress. For example, both NFE2L1 and NFE2L2 bind promoters for genes encoding glutathione S-transferase (GST) and glutathione peroxidase (GPX1) (Bugno *et al*., 2015) However, NFE2L1 does have functions relating to ARE that cannot be compensated for by NFE2L2. Cui and colleagues (2017) demonstrated in a MIN6 pancreatic β cell model that NFE2L1-deficiency sensitizes the cell to apoptosis in acute arsenite exposure, demonstrating a parallel but crucial function of NFE2L1 in complementing those of NFE2L2. In a keratinocyte model, NFE2L1 expression was demonstrated to be protective against ultraviolet light exposure; its inhibition led to increased activation of BCL-2-mediated apoptosis (Han *et al*., 2012). Thus, NFE2L1 is a critical component of the antioxidant response as, even under generalized oxidative stress conditions, its function appears crucial to cell survival.

NFE2L1 knockout appears to be embryonically lethal in mice and human embryonic cells. Conversely, NFE2L2 knockout is not. This points to an important distinction between these two proteins of parallel functionality (Jennings *et al*., 2012). However, stable NFE2L1 knockout cancer cell lines have since been established (Zhu *et al*., 2020). Reduced expression of NFE2L1

has been characterized as increasing the vulnerability of cells to stressors. For example, NFE2L1 knock down has been shown to increase pancreatic β-cell vulnerability to arsenite cytotoxicity (Cui et al., 2017). NFE2L1 deficiencies have also been linked to increased ER stress in liver model systems, which has been associated with the development of organ-specific pathologies. Further, NFE2L1 knockout in adult mice has been shown to lead to liver steatosis, inflammation and tumorgenesis (Kim et al., 2016). This pathogenesis is certainly not solely linked to the possible role of NFE2L1 in the UPR – NFE2L1 is well-established as binding the antioxidant response element and oxidative stress is also a staple of liver disease progression – but the concordance of these two factors nonetheless warrants further investigation (Kim et al., 2016).

Recently, it has been suggested that NFE2L1 may be regulated by mTORC1 through activation of sterol-regulatory element binding protein family of transcription factors (SREBP1), which bind the NFE2L1 promoter. These signals are described as intrinsic, or mediated by extracellular signals detected by mTORC1. Further, SREBP1 was shown to bind the NFE2L1 promoter, and not that of NFE2L2; yet another mechanism of action differentiating it from other CNC proteins (Zhang & Manning, 2015).

There are shorter isoforms including p85, p65, p55, p46, p36 and p25 (Bugno *et al*., 2015). The 85kDa isoform is a transcriptional activator of genes controlled by NFE2L1, but all smaller isoforms are inhibitors of other CNC family proteins. By inhibiting CNC family treanscription factors, these isoforms of NFE2L1 act as potent repressors of ARE activation (Bugno *et* al., 2015) Other distinct isoforms of NFe2L1 include Nrf1D and Nrf1ΔS. Not much is known about Nrf1D apart from the fact that it is a secretory protein found in blood plasma; Nrf1ΔS is an alternative splice variant of Nrf1D (Yuan *et al*., 2018; Bugno *et al*., 2015).

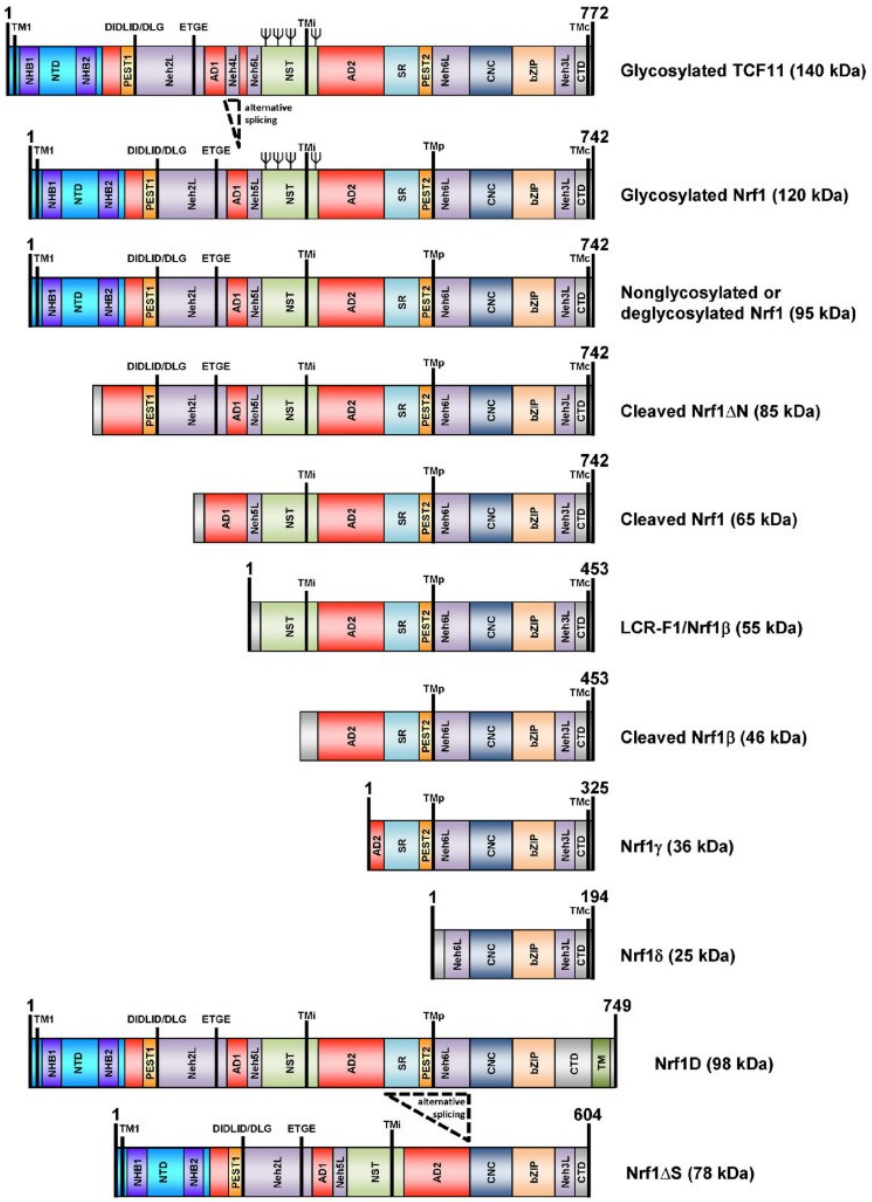

Figure 2 Isoforms of NFE2L1. Figure is modified from Zhang and Hayes 2013.

The last of the nuclear factor erythroid 2-like CNC bZIP transcription factors is NFE2L3. Similarly to NFE2L1, when heavily glycosylated, it is bound to the ER membrane. Deglycosylated NFE2L3 is also released into the cytoplasm and acts as a transcription factor in the nucleus (Chevillard & Blank, 2011). Its functions have yet to be fully delineated, though recent evidence suggests it acts in complement to NFE2L1 functions as it relates to proteasome synthesis (Waku *et al*., 2020).

Beyond its role in responding to oxidative stress, the p95 isoform of NFE2L1 (hereafter simply referred to as NFE2L1) is also responsible for responding to disruptions to proteostasis. Of the CNC bZIP transcription factors, NFE2L1 most strongly enhances the expression of proteasomal subunits – 6 times greater capacity in this role than NFE2L2 (Steffen *et al*., 2010). Proteasomal inhibitors strongly activates the NFE2L1-controlled expression of both the 19S regulatory complex and the 20S core of the 26S proteasome (Kim *et al*., 2016). The mechanism through which NFE2L1 is activates in proteasomal inhibition requires further study. However, due to the robust response resulting from this stressor, and the unknown nature of its activation, the notion that NFE2L1 may be a sensor of proteotoxic stress is currently being investigated (Jennings *et al*., 2012). Because of its role in these cellular survival mechanisms, NFE2L1 has been implicated in a variety of cancers, where oxidative and proteotoxic stresses are common (Brehme *et al*., 2019). Proteasomal inhibitors are common in cancer therapeutics, and NFE2L1 expression is related to resistance to such treatments. NFE2L1 knock down has been demonstrated to sensitize cancer cells to dual treatment of proteasomal inhibitors and chemotherapy (Tomlin *et al*., 2017) In fact, recent work has claimed that NFE2L1 expression is essential for cancer cell growth, and further that NFE2L3, the closest CNC-family protein homolog to NFE2L1, may compensate to some degree in promoting proteostasis in cancer cells

(Waku *et al*., 2020; Sherman & Li, 2020).

1.4 NFE2L1 and the Unfolded Protein Response

Parallel functions have been observed between NFE2L1 activity and that of the UPR. An integral function of the UPR is to promote the ubiquitination and degradation of misfolded proteins through ERAD signaling, with XBP1 as the primary transcription factor effector in the process (Hetz, 2012). Given NFE2L1 is an important transcription factor in promoting the expression of proteasomal subunits, which combined perform a function that is crucial to effective ERAD, the possibility that NFE2L1 may play a role in the UPR warrants investigation. Several other similarities have been observed between NFE2L1 functionality and that of the UPR over the years. One such link between NFE2L1 and the UPR is their mutual regulation of the protein synoviolin/hrd1, an ER-membrane-spanning E3 ubiquitin ligase which inactivates IRE1α and targets membrane-bound NFE2L1 for proteasome-mediated degradation (Li *et al*., 2015; Kim *et al*., 2016). In the UPR, this is thought to serve as a negative feedback loop in controlling IRE1α expression to prevent apoptotic signaling in acute and chronic ER stress conditions. It may also play a negative feedback roll to mediate the expression of NFE2L1. Further, synoviolin is also involved in the ubiquitination of misfolded proteins as part of the UPR. NFE2L1 is essential for the regulation of synoviolin, protecting the cell from ER-stress-related cell death. NFE2L1 knock down in PC-12 cells abolished ER stress-related induction of synoviolin, and significantly reduced cell viability under ER stress conditions (Li *et al*., 2015). To complicate matters further, NFE2L1 binds an ARE in the promoter of homocysteine-and-ER stress-inducible, ubiquitin-like domain member 1 (Herpud1), an ERAD effector protein which

targets synoviolin for ubiquitination and degradation (Ho & Chan, 2015). NFE2L1 modulates the expression of ubiquitin ligases as part of promoting cell survival through the degradation of IRE1α, but also in the negative regulation of that very same pathway to maintain ERAD signaling. These results strongly implicate NFE2L1 in UPR signaling via modulation of IRE1α degradation and ERAD effectors.

Though tunicamycin and thapsigargin cause ER stress and do not activate NFE2L1, proteasome inhibition causes ER stress and a robust UPR activation, and strongly induces NFE2L1 activation (Sha & Goldberg, 2014). Further, inhibition of NFE2L1 results in ER stress (Zhu *et al*., 2020). As such, the association between NFE2L1 and ERAD is unidirectional; disruptions to calcium and glycosylation equilibrium in the ER, resulting in ER stress, do not activate NFE2L1. The proteasome is, however, an essential part of ERAD. Recently, Zhu and colleagues demonstrated that NFE2L1 has the ability to bind strongly to an ARE within the XBP1 promoter, strongly suggesting a role in promoting its UPR activity (Zhu *et al*., 2020). This requires further investigation.

More evidence linking NFE2L1 to the UPR can be gleaned from studies investigating the effects of proteasome inhibitors on NFE2L1 expression, and their effects on the UPR. Acute exposure to proteasome inhibitors can lead to terminal, pro-apoptotic UPR signaling. In cancer therapy, proteasome inhibitors have proven a reasonably effective treatment for patients suffering with multiple myeloma. However, in other cancers, proteasome inhibition has demonstrated limited effectiveness at tolerable doses. This is thought to be, in part, due to the "bounce back" effect of proteasome inhibitors insofar as they strongly induce NFE2L1, which enhances the production of proteasome subunits, compensating for the inhibition from the treatment. Given this, combinatorial treatments have been suggested wherein proteins which

ordinarily process NFE2L1 into its active form, such as DDI2 and NGLY1, may reduce the "bounce back" effect of proteasome inhibitor treatments, enhancing pro-apoptotic UPR signaling (Sherman & Li, 2020; Koizumi *et al*., 2016; Kobayashi & Waku, 2020). This treatment methodology implies that NFE2L1 is important in proteostasis and enhances cell survival as part of ERAD. No mechanistic links are implied, but NFE2L1 appears to be important to this critical, pro-survival UPR function. Lee and colleagues demonstrated that myeloma cells treated for 4 hours with the proteasome inhibitor MG-132 demonstrated a highly disrupted UPR signaling. This affected XBP1(S) in particular; increased concentration of MG-132 demonstrated a strong inhibition of XBP1(S) and stabilization of the normally degraded XBP1(U). They also generated a stable XBP1(U) mutant to imitate the effect of the proteasome inhibitor on XBP1(U) specifically, and found the same decrease in XBP1(S) production (Lee *et al*., 2003). From this study, it is observed that disruption in proteasome expression can have a negative effect on XBP1(S) ERAD signaling through the stabilization of XBP1(U). It is plausible, then, that inhibition of NFE2L1 and the resulting disruption of proteasomal subunit synthesis may also stabilize XBP1(U), inhibiting XBP1(S) ERAD signaling. The combined treatment with MG-132 and the ER stressor thapsigargin resulted in a further decrease in cell viability than observed when treated with MG-132 alone. The stabilization of XBP1(U) is of particularl interest as it has been demonstrated to be an inhibitor of its active splice variant (Yoshida *et al.*, 2006). Under normal conditions, XBP1(U) is quickly degraded by the proteasome under ubiquitin dependent and independent mechanisms (Tirosh *et al*., 2006). In the late-stage recovery phase of ER stress, however, XBP1(U) accumulates, and complexes with XBP1(S). XBP1(U) possesses a nuclear exclusion domain and thus the XBP1(S)/XBP1(U) complex cannot enter the nucleus, inhibiting the transcription factor activity of XBP1(S). Further, the C-terminal degradation signal of

XBP1(U) triggers the degradation of the entire complex (Yoshida *et al*., 2006). XBP1(U) also binds active ATF6 protein (Yoshida *et al*., 2009). This negative feedback isoform of XBP1 may be stabilized by the inhibition of the proteasome by MG-132, inhibiting the effectors of the IRE1α and ATF6 branches of the UPR. Thus, ER stress is induced as a result of the accumulation of undegraded proteins, but the UPR ERAD pathway cannot be initiated (Lee *et al*., 2003). Given this, one mechanism by which NFE2L1 may be important in the UPR is by enhancing the expression of proteasomal subunits to degrade the inhibitory unspliced isoform of XBP1.

1.5 Research Goals

Given the apparent similarities in function between the UPR and NFE2L1, the goal of our research is to establish whether the latter possesses regulatory functions of the former, or if they are truly simply parallel in function in the restoration of proteostasis.

To do this, we will observe the relative expression of XBP1 splice variants in response to NFE2L1 overexpression and knock down in ER stress conditions. As previously discussed, XBP1 is the primary effector transcription factor of the IRE1α branch of the UPR. In conditions of ER stress, its nascent RNA is spliced, enabling the translation of the active transcription factor variant. The unspliced variant demonstrates a very short half-life, but is nonetheless observable under stable conditions, though it is rapidly degraded under ER stress conditions. Conversely, the expression of the spliced isoform increases significantly under such conditions (Hetz, 2012). By observing the relative change in expression of each isoform, the activation of the UPR can be assessed under various circumstances. To date, the relationship between XBP1 isoforms has not

been sufficiently investigated, as it relates to NFE2L1 expression at the gene of protein level. We will observe whether the overexpression or knock down of NFE2L1 influences the expression, and processing, of the XBP1(U) and XBP1(S) isoforms, and whether this has an impact on UPR signaling under ER stress conditions.

Our hypothesis is as follows: the overexpression and knock down of NFE2L1 will alter the splicing of nascent XBP1(U) RNA into its active (XBP1(S)) splice variant. Specifically, we predict that knock down of NFE2L1 will decrease the amount of XBP1(S) RNA and/or protein produced under ER stress conditions, and that overexpression of NFE2L1 will enhance the production of the active transcription factor variant.

Our first objective is to find whether or not the overexpression or knockdown of NFE2L1 alters the splicing of XBP1 under ER stress conditions. If our results relating to our first objective are in line with our hypothesis, our second goal will be to ascertain the level as which NFE2L1 plays a role in this branch of the UPR; to achieve this, we will be observing XBP1 splicing at the level of protein and RNA.

To achieve these objectives, we have acquired a HCT116 cell line stably transfected with a plasmid which, in response to ER stress; this cell line translates a spliced XBP1-mNeonGreen fusion protein as part of its UPR (Nougarède *et al*., 2018). Thapsigargin treatment will be applied to this cell line in both NFE2L1 knock down and overexpression conditions to observe the efficacy of XBP1(S) synthesis in both fluorescence microscopy and flow cytometry. Further, Western blotting was performed using an antibody that detects both the spliced and unspliced variants of XBP1, as well as to observe the overexpression and knock down of NFE2L1 on both protein isoforms. Finally, the relative RNA expression of each XBP1 isoform will be quantified

under similar conditions of NFE2L1 expression modulations using real-time quantitative polymerase chain reaction (RT-qPCR).

We focused on XBP1 rather than other UPR effectors, for various reasons. Most importantly, the interplay between the splice isoforms is unique in XBP1; more dynamic than observing the altered expression of other individual UPR effectors. Among the three branches of the UPR, the IRE1α branch is the most highly conserved evolutionarily, being present in all eukaryotes (Tsuru *et al*., 2016). Additionally, the UPR converges on the splicing of XBP1, and is thus changes in the UPR in all three branches of the UPR will alter XBP1 expression. The processed, active ATF6 transcription factor binds the XBP1 promoter, enhancing its expression (Yoshida *et al*., 2001). Further, the final transcription factor produced from PERK activation of the UPR, ATF4, binds the promoter of IRE1α and enhances its expression. In fact, inhibition of the PERK branch of the UPR results in the inhibition of *de novo* IRE1α expression under ER stress conditions (Tsuru *et al*., 2016).

The null hypothesis would state that there is no link between NFE2L1 expression and XBP1 alteration (either gene or protein expression or splicing); RNA and protein expression of XBP1 isoforms in control and ER stress conditions will be similar under negative control conditions as well as NFE2L1 overexpression and knock down. To reject this hypothesis, the number of cells exhibiting fluorescence of the XBP1(S)-mNeonGreen fusion protein would have to be altered under conditions of NFE2L1 overexpression and knock down when treated or untreated. Further, this change in expression pattern would alter the abundance of each isoform in Western blot analysis. Finally, the relative change of XBP1 RNA in both isoforms would be disrupted under thapsigargin treatment.

The UPR is implicated in a variety of pathologies relating to the accumulation of misfolded proteins (Voisine *et al*., 2010). Many cancers have found in the UPR a useful tool in promoting cell survival in the harsh conditions inherent to tumor microenvironment. If NFE2L1 is affiliated by the UPR, it may present an interesting therapeutic target for the enhancement of diminishing of the UPR as is advantageous to a given pathology. Because of its complicated activation, there exist multiple potential targets to control the expression of genes controlled by NFE2L1, such as NGLY1 and DDI-1/2 (Koizumi *et al*., 2016; Tomlin *et al*., 2017; Kim *et al*., 2016).

Chapter 2: Materials and Methods

2.1 Cell Lines

Human colorectal cancer cell lines HCT116 from the American Tissue Culture Collection (ATTC, Manassas, Virginia) were cultured in complete media consisting of McCoy's 5A medium (Sigma-Aldrich, St. Louis, Missouri, U.S.A.) supplemented with 10% fetal bovine serum (FBS) (Gibco/Thermo Fisher Scientific, Waltham, Massachusetts, U.S.A.), at 37°C, 5% CO_2, 21% O_2 in a Thermo Forma Series II Incubator (Waltham, Massachusetts, U.S.A.). Cells were passaged every 3 days by removing media, washing with sterile phosphate buffered saline (PBS) and dissociate from the substrate using 0.25% Trypsin in PBS (Gibco/Thermo Fisher Scientific Waltham, Massachusetts, U.S.A.) for under 5 minutes. Trypsinization was terminated with a volume of complete McCoy's media containing 10% serum 9 times greater than that of

the trypsin. The trypsin was then removed from the media by centrifugation of the cells and resuspension in media.

- *XBP1(S)-mNeon Green HCT116 Cells*

A subset of HCT116 cells were designated for lentiviral transfection of a linear, double-stranded DNA pLVx vector with a sequence cloned therein that would produce XBP1(S) protein conjugated with mNeon Green. This cell line was prepared by a member of the Andrews lab at the Sunnybrook Research Institute and sent to the McKay lab at Carleton University, which was then shared with the Willmore lab. This was done according to a protocol by Nougarede *et al.* (2018). When treated with an ER stressor, the fluorescent marker is observable by fluorescence microscopy, and adequate for flow cytometry analysis. The mNeonGreen protein conjugated to XBP1(S) was situated after the stop codon for the unspliced variant; the frameshift that occurs when translating the spliced variant enables the synthesis of the fusion protein containing the fluorescent marker.

2.2 Chemical Treatments

To induce ER stress, cells were treated with 300 nM thapsigargin (Cayman Chemical, Ann Arbor, Michigan, U.S.A.), a phytochemical ER-membrane SERCA Ca^{2+} pump inhibitor. The 1.5 mM thapsigargin stock is diluted down to 300 nM (final concentration) in complete media supplemented with 10% FBS. Media in each well, containing transfection reagent, was substituted for media with or without the thapsigargin treatment.

2.3 Lipid-Based Transfections

2.3.1 Oligofectamine™ (RNAi)

DsiRNA transfections for NFE2L1 knock down were performed in accordance with the Oligofectamine™ protocol (Invitrogen/Life Technologies/ThermoFisher Scientific, Waltham, Massachusetts, U.S.A.). According to the procedure outlined by the manufacturer, the Oligofectamine reagent was equilibrated in serum-free McCoy's media for 10 minutes, vortexed for 5 seconds every 2 minutes. dsRNAi oligonucleotide (20 μM) was separately combined with serum-free McCoy's media. The two above solutions were combined and incubated at room temperature of 20 minutes, vortexing every 5 seconds for 3 minutes. This final preparation was then combined with the cells in serum-free McCoy's media and the transfection was allowed to take place over 6-8 hours, at which point the media was supplemented with serum. The efficiency of dsRNAi transfection was established by real-time quantitative polymerase chain reaction (RT-qPCR), where change in relative expression represents the percentage of cells exhibiting the knock down ((1/ 2^dCq)*100).

2.3.1.1 RNAi Oligonucleotides

The oligonucleotides used for RNA interference of NFE2L1 are shown below, with "r" designating a ribonucleotide (as opposed to a deoxyribonucleotide which is shown without the "r" preceding it):

- NFE2L1:
    - Sense 5' GGCGUGAGGUUUUUGACUAUAGUCA 3'
    - Antisense 5' UGACUAUAGUCAAAAACCUCACGCCCA 3'
- The Negative Control utilized for RNA interference is shown below. This Negative Control has been tested to ensure that it does not have off-target knock downs of other genes.
    - Integrated DNA Technologies Universal Negative Control. Ref. #: 51-01-14-03

2.3.1.2 Double Transfection

In a conventional transfection, the solution of transfection reagent and dsRNAi in serum-free media is added to a dish of previously seeded cells adherent to the substrate of a dish or plate. In a reverse transfection, cells in suspension in serum-free media are added into a well containing the transfection reagents. In a conventional transfection, transfection reagents and serum-free media are added to a well containing cells adhering to the well substrate. For the double transfection protocol, cells were initially reverse-transfected for 6-8 hours, then allowed to grow in media containing serum for 24 hours, and then subjected to a conventional transfection for 6-8 hours, then either immediately treated with 300nM thapsigargin for 16 hours,

or allowed to grow in serum media for 8 hours prior to a 6-hours treatment with thapsigargin (Liu *et al*., 2004; Erfle *et al*., 2007; Okazaki *et al*., 2007).

2.4 Lipofectamine LTX (Plasmid)

Plasmids were purified from bacteria using a Wizard Plus DNA Purification system (Promega, Madison, Wisconsin). Plasmid transfections for NFE2L1 overexpression (pCR3.1-FLAG-NFE2L1) were performed in accordance with the Lipofectamine LTX^{TM} protocol (Invitrogen/Life Technologies/ThermoFisher Scientific, Waltham, Massachusetts, U.S.A.). Plasmid and LTX reagent were incubated in Opti-MEM (Gibco/ThermoFisher Scientific, Waltham, Massachusetts, U.S.A.) reduced serum media for 30 minutes at room temperature, vortexing for 5 seconds every 3 minutes. Cells were reverse-transfected for 6-8 hours in serum-free Opti-MEM media and subsequently supplemented with serum. The number of cells reverse-transfected was equivalent to 80% confluency in the well, or approximately $7.6x10^5$ cells in a flat-bottom 6-well plate. Media was substituted with McCoy's media 8 hours later. Double-transfections were not performed as this resulted in reduced in excessive cell death and low transfection efficiency. Transfection efficiency was assessed by transfecting a plasmid encoding GFP into HCT116 cells and counting GFP-positive cells by fluorescence microscopy using a EVOS FL Cell Imaging System (Invitrogen/Life Technologies/ThermoFisher Scientific, Waltham, Massachusetts, U.S.A.). The negative control plasmid used was a PUC19 empty cloning vector.

2.4.1 Plasmids

The plasmid used to overexpress N-terminal FLAG-tagged NFE2L1 was created in the mammalian expression vector pCR3.1 (Chepelev et al., 2011). This expression vector has had the NdeI site in the CMV promoter mutated to PmlI, to allow for the cloning of any gene using NdeI site (the only restriction site with ATG in frame) as a fusion to FLAG. The NdeI to PmlI alteration was in a non-essential region of the CMV promoter and did not affect the expression of genes cloned into the altered pCR3.1 plasmid. The negative control plasmid used for transient transfection of mammalian cells was a PUC19 empty cloning vector.

2.5 Fluorescence Microscopy

Using the XBP1 fluorescent HCT116 variant cell line, fluorescence microscopy was performed using a EVOS FL Cell Imaging System (Invitrogen/ Life Technologies/ThermoFisher Scientific, Waltham, Massachusetts, U.S.A.). The microscope possesses the ability to overlay images acquired using mNeonGreen fluorescence detection with images acquired using conventional bright-field microscopy in the integrated software. Further, cell counts for cells positive or negative for mNeonGreen fluorescence were also collected using integrated software. To ensure negligeable background fluorescence, the relative brightness of the overlayed brightfield and fluorescence images were adjusted for maximum clarity and no green colour in micrograph quadrants devoid of cells. Cells considered positive for XBP1(S) expression were those exhibiting a single, moderately bright green circle within the cell's boundary, likely representing nuclear localization of the XBP1(S) transcription factor. Images were acquired at

100X magnification after either 7- or 16-hours following media substitution with McCoy's complete media supplemented with 10% FBS containing 300 nM thapsigargin.

2.6 Flow Cytometry

Flow cytometry was exclusively performed on the HCT116 variants expressing the mNeonGreen-conjugated XBP1(S). Prior to running through the flow cytometer, all samples were prepared as follows; media was removed from each well, residual media was washed off of cells with 1 X sterile PBS, cells were trypsinized (0.25% trypsin) for 3-5 minutes, trypsinization was stopped with a volume of serum-supplemented media three-fold that of the trypsin, cells were centrifuged 900 X g for 5 minutes, media with residual trypsin was removed, cells were resuspended in flow buffer (0.5% BSA, 2mM EDTA in PBS), centrifuged again at 900 X g for 5 minutes, flow buffer was decanted, and cells were resuspended a second time in flow buffer. Each sample was pipetted up and down 5 times immediately prior to loading into a flat-bottom, non-adherent 96-well plate. The flow cytometer used was the BD Accuri C6 Flow Cytometer (BD Biosciences, Franklin Lakes, New Jersey, U.S.A.). Treated cells were incubated with 300nM thapsigargin for 12 hours to ensure maximal fluorescence from the reporter. The flow cytometer detected the relative green fluorescence of individual cells and the plot of cell count vs. relative fluorescence was collected in BD Accuri C6 Analysis Software (BD Biosciences, Franklin Lakes, New Jersey, U.S.A.).

2.7 Western Blot

XBP1(S/U) and NFE2L1 protein expression were measured by Western blot. Gels consisted of 15% acrylamide for XBP1(U/S) blots and 8% for NFE2L1. All gels contained 28 µL 30% ammonium persulphate and 8 µL TEMED for polymerization, and 0.1% 2-2-2-Trichloroethanol (TCE) for stain-free protein loading normalization. Protein was harvested in 1 X radioimmunoprecipitation assay (RIPA) lysis buffer (50 mM Tris HCl, 150 mM NaCl, 1.0% (v/v) NP-40, 0.5% (w/v) sodium deoxycholate, 1.0 mM EDTA, 0.1% (w/v) SDS and 0.01% (w/v) sodium azide at a pH of 7.4; Pierce, ThermoFisher Scientific Ottawa, Ontario, Canada), and quantified using the Pierce™ BCA colorimetric assay (ThermoFisher Scientific, Ottawa, Ontario, Canada). After quantification, protein in RIPA was mixed 1:1 in 2 X Laemelli buffer supplemented with sodium dodecyl sulfate for protein denaturation to linear confirmation. The final protein denaturation step was to heat the above mixture to 95°C for 3 minutes. Total protein (16 µg) was loaded into each well of a 15-well, 1.5 mm wide gel. The molecular weight standard used was 10 µL of the Bio-Rad Precision Plus Protein™ All-Blue Ladder (Hercules, California, U.S.A.) Gel electrophoresis was run at 120 V for 180 minutes. Following SDS-PAGE, loading normalization was performed by TCE stain-free imagine of gel in transfer buffer using Bio-Rad Molecular Imager Gel Doc System (Hercules, California, U.S.A.). Polyvinylidene difluoride (PVDF) membrane was then activated in 100% methanol and equilibrated in transfer buffer (20 mM Tris-HCl (pH 8.0), 150 mM glycine, 20% methanol) for 5 minutes prior to start of transfer of protein onto membrane. Wet transfers were run overnight at 180 mA at 4°C. Once the transfer was complete, the membrane was blocked in TBST (20 mM Tris-HCl (pH 7.6), 137 mM NaCl, 0.1% Tween-20) containing 10% w/v fat-free milk powder for 60 minutes at room temperature. The blocking solution was washed off with TBST and the membrane exposed to primary

antibody (XBP1(U/S) (antigen: region within residues 100 and 250; Novus Biologicals NBP1-77681); NFE2L1 (antigen: residues 192-253; Novus Biologicals NBP2-55915) for 90 minutes at room temperature. The membrane was washed 3 times for 5 minutes using TBST before the membrane was exposed to secondary antibody for 60 minutes at room temperature. The membrane was then washed 3 times for 5 minutes using TBST. A 1:1 mixture of each reagent in the Bio-Rad Clarity™ Western ECL Substrate (Bio-Rad Hercules, California, U.S.A.), and pipetted gently onto the washed membrane, allowed to incubate at room temperature for 10 minutes prior to chemilumiescent imagine using the Bio-Rad Molecular Imager Gel Doc XR+ System (Bio-Rad, Hercules, California, U.S.A.).

2.7.1 Densitometry

Quantification of the density of Western Blot bands was performed using Image Lab 6.0 software (Bio-Rad, Hercules, California, U.S.A.). Densitometry was measured in individual bands in equal-sized boxes across the blot, in each lane. The integrated density value of each band was normalized using total lane volume of the TCE stain-free image.

2.8 RNA Isolation, cDNA Synthesis

Harvested cells were flash-frozen in liquid nitrogen and stored at -80°C prior to total RNA isolation. Samples were homogenized from the frozen state, and total RNA was extracted using the Bio-Rad Aurum™ Total RNA Mini Kit (Bio-Rad, Hercules, California, U.S.A.) using the Spin protocol, where samples are centrifuged at 4°C. RNA was quantified by Nanodrop using

a DeNovix DS-11 Spectrophotometer (DeNovix, Wilmington, Delaware, U.S.A.), and 1 µg of total RNA was reverse transcribed to cDNA using the iScript™ cDNA synthesis kit by Bio-Rad (Hercules, California, U.S.A.). The resulting cDNA was diluted in deionized, nuclease-free water 1/64 to 15.625ng/µL. Normalization for reverse-transcription efficiency variability was later done by GAPDH qPCR.

2.9 RT-qPCR

All qPCR runs were performed using 10 µL reactions using the Bio-Rad (Hercules, California, U.S.A.) These reactions consisted of 4 µL cDNA template (15.625ng/µL), 5 µL SsoAdvanced™ universal SYBR Green Supermix from Bio-Rad (Hercules, California, U.S.A.), and 0.5µL of each forward and reverse primer in a given set. All primer sets had unique annealing temperatures and thus all samples were run separately with each set. Triplicate no-template-control samples (deionized water "template") were run each time to ensure there were no contaminants.

2.9.1 RT-qPCR Primers

Table 1: Primer list for RT-qPCR

Name	Accession no.	Forward Primer	Reverse Primer
XBP1	NM_001079539.1	5' GAGCCAAGCTAATGTGGTAGT 3'	5' GAGGTCATCTTCTACAGGTTCTTC 3'
	NM_005080.3	5' CTCAGACTACGTGCACCTCT 3'	5' TGAATCTGAAGAGTCAATAC 3'
GAPDH	NM_002046.7	5' CTTTGGTATCGTGGAAGGACTC 3'	5' GAGGCAGGGATGATGTTCTG 3'
NFE2L1	NM_003204.3	5' CTGGAGGAGGAATTTGACTCTG 3'	5' TTCTTCCTCCTCCTCTTCCTC 3'

The reaction efficiencies for each set of primers were optimized. Primarily, the primers were run with a given sample predicted to contain a large amount of cDNA specific to the primer set on a gradient with a temperature range of 12°C. Once a range of temperatures were identified as strongly amplifying a single product (as verified on a using melt curve analysis), the experiment was repeated with greater resolution: a temperature range of 3°C. Once the optimal annealing temperature was established, reaction efficiency was assessed using a serial dilution of template and assessing the concordance in regression analysis (R^2 value). All primers were optimized for >98% reaction efficiency.

RT-qPCR was carried out using the Bio-Rad CFX Connect Real-Time System (Bio-Rad. Hercules, California, U.S.A.). All samples were run in accordance with the SsoAdvanced™ protocol, varying only in annealing temperature specific to a given set of primers. All samples were run for 35 cycles; samples that did not amplify beyond the threshold by the 32nd cycle were considered null of amplicon. Beyond the 35-cycle run, a melt curve analysis was performed between on each sample amplified with a given set of primers to ensure a unique, intended

amplicon product. Amplification threshold was set in the early exponential phase to ensure the highest sensitivity. Data was collected, amplification threshold set, melt curve scrutinized, and data analyzed in Bio-Rad CFX Maestro^{TM} software (Bio-Rad, Hercules, California, U.S.A.).

2.10 Statistical Analysis

Statistical analysis was performed in SigmaStat software and graphs were generated in SigmaPlot (Systat, San Jose, California, U.S.A.). This was done by one-way ANOVA tests followed by post-hoc analyses including Dunnett's tests. Analyses comparing the negative control, untreated sample to others was performed by Dunnett's test. Comparisons between treatment groups not including the untreated negative control were performed using Tukey's tests. All figures display the mean values from each treatment groups, with error bars corresponding to standard error of the mean (SEM). Replicates were technical replicates of the HCT116 cell line analyzed on different days. Statistical significance annotations on figures are always based on the following: N.S. – non-significant; * - $p<0.05$; ** - $p<0.01$; *** - $p<0.001$.

Chapter 3: Results

3.1 Fluorescence Microscopy of HCT116 cells expressing mNeonGreen-conjugated XBP1(S)

3.1.1 DsRNAi-mediated NFE2L1 Knock down

HCT116 cells expressing mNeonGreen-conjugated XBP1(S) were double transfected (1 reverse, 1 conventional) with dsRNAi oligos targeting NFE2L1 RNA for degradation via association with RISC nuclease complex. Following a 6-hour incubation with 300 nM thapsigargin, the number of cells positive for strong expression of the mNeonGreen-fluorescent cells was compared across knock down versus negative control, as well as untreated versus treated.

It was observed that untreated cells, under both standard and NFE2L1 knock down conditions, exhibited the same relative XBP1(S) fluorescence: 5.0±0.94% and 5.37±1.35%, respectively (N.S.; $p > 0.05$). In cells transfected with the negative control oligo, XBP1(S) positivity increased significantly when treated with 300 nM thapsigargin for 6 hours to 48.9±0.62% ($p \leq 0.001$). When knocked down with the dsRNAi oligo, cells did not exhibit the same increase in fluorescence relative to the knock down untreated ($p > 0.05$) or the negative control untreated cells ($p > 0.05$). Further, the fluorescence of the negative control cells treated with thapsigargin was significantly higher than knocked down cells treated similarly ($p \leq 0.05$; Fig. 1B)

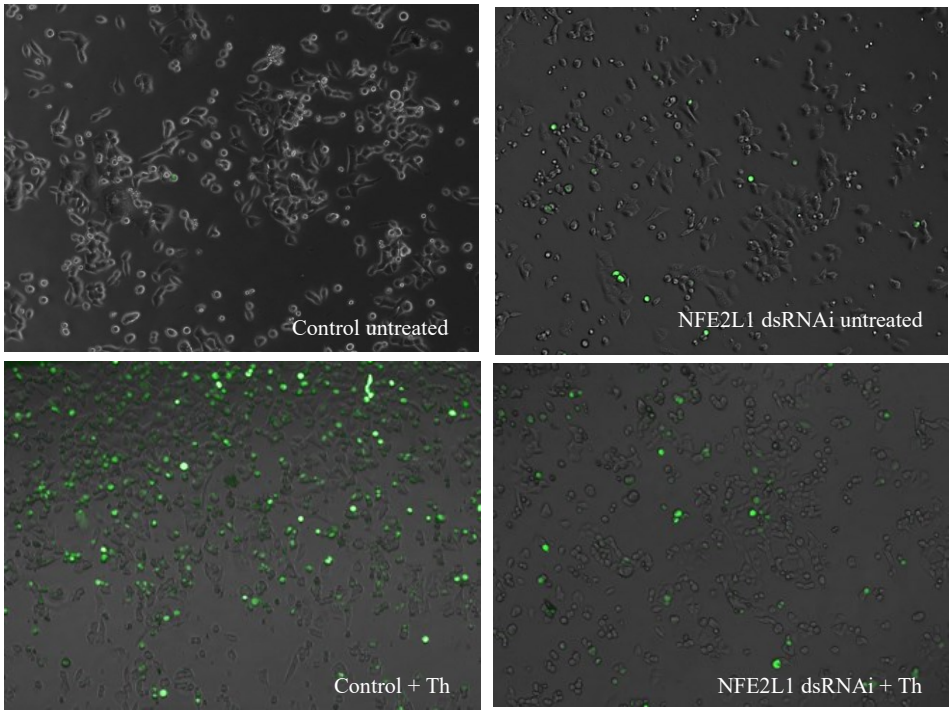
Control untreated
NFE2L1 dsRNAi untreated
Control + Th
NFE2L1 dsRNAi + Th

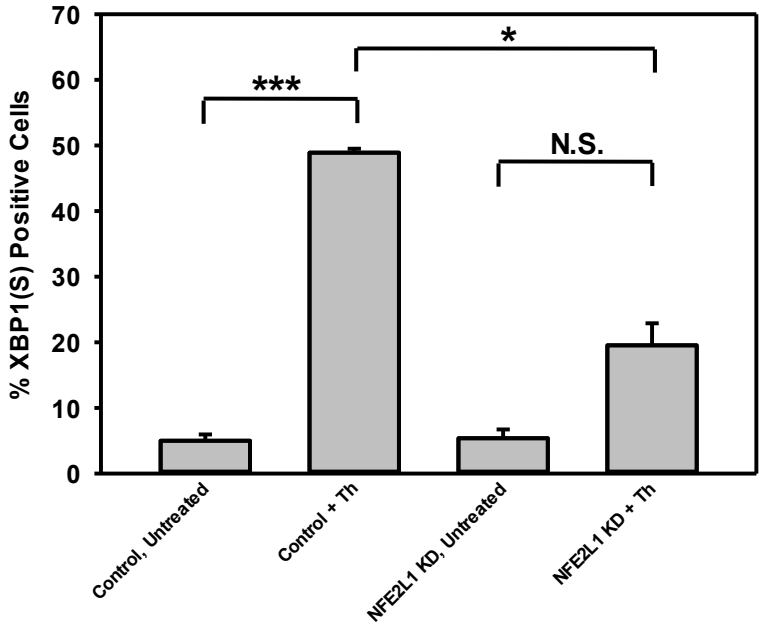
% XBP1(S) Positive Cells
70
60
50
40
30
20
10
0
***
*
N.S.
Control, Untreated
Control + Th
NFE2L1 KD, Untreated
NFE2L1 KD + Th

Figure 3: HCT116 Cells positive for XBP1(S) expression in NFE2L1 RNAi-mediate knock down, thapsigargin treatment. HCT116 cells expressing the mNeonGreen-conjugated XBP1(S) protein were double-transfected with either a negative control or NFE2L1-targeting dsiRNA oligonucleotide using the Oligofectamine reagent. Media was substituted 6 hours prior to analysis; control media contained 0.01% DMSO (v/v) and treatment media contained 300nM thapsigargin (Th). (A) Photomicrographs of each treatment condition (B) Graphical representation of % cells positive for fluorescent XBP1(S). The data represents mean ± S.E.M. Tukey's test analysis: *** $p<0.001$; * $p<0.05$; N.S. non-significant. N=3.

3.1.2 Plasmid-mediated NFE2L1 Overexpression

HCT116 cells expressing the mNeonGreen-conjugated form of XBP1(S) were subject to a single reverse transfection of a plasmid overexpressing FLAG-tagged NFE2L1. XBP1(S) fluorescence was assessed by counting cells exhibiting intense green fluorescence across treatment groups transfected blank/overexpressing and untreated/treated for 6 hours with 300 nM thapsigargin.

Under conditions of NFE2L1 overexpression, the untreated sample demonstrated a significantly increased XBP1(S)-positive cell count compared to the transfected control sample; 3.63±0.52 in transfected control and 33.87±5.79% when overexpressing NFE2L1 ($p\leq0.05$). Treatment with thapsigargin resulted in a significant increase in XBP1(S) positivity in both control and overexpressing samples; 3.63±0.52 to 41.03±2.93% and 33.87±5.79% to 59.93±5.92%, respectively (both $p\leq0.05$). The transfected NFE2L1-overexpressing sample treated with thapsigargin did not show statistically significant increased XBP1(S) positivity relative to the transfected control cells under the same treatment ($p>0.05$; Fig. 2B)

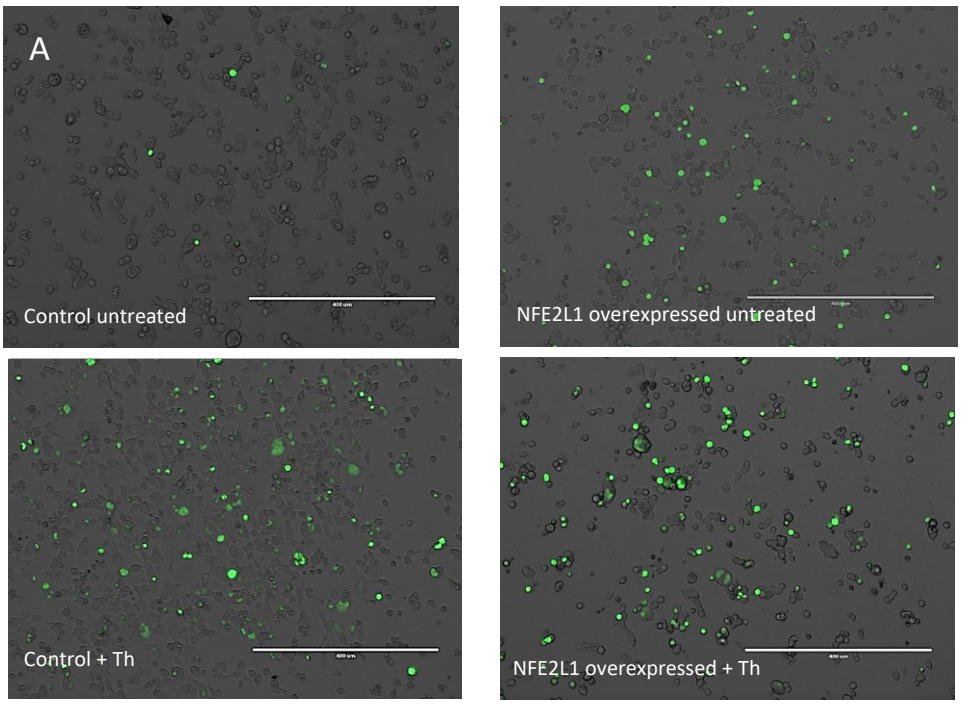
A
Control untreated
NFE2L1 overexpressed untreated
Control + Th
NFE2L1 overexpressed + Th

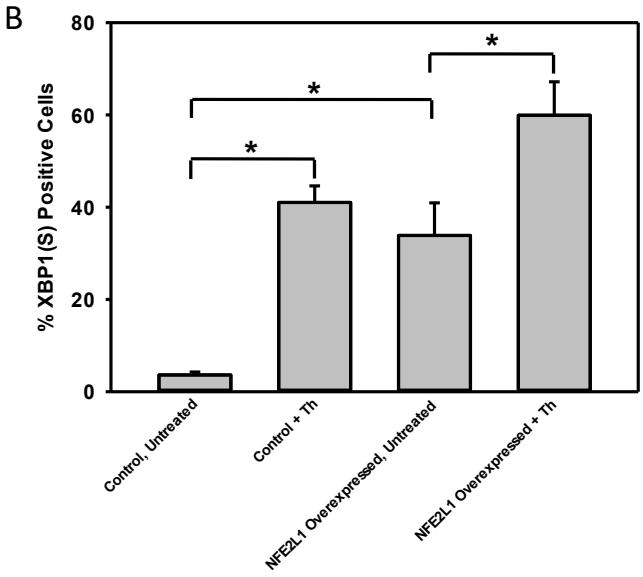
B
% XBP1(S) Positive Cells
80
60
40
20
0
*
*
*
Control, Untreated
Control + Th
NFE2L1 Overexpressed, Untreated
NFE2L1 Overexpressed + Th

Figure 4: **HCT116 Cells positive for XBP1(S) expression in NFE2L1 Plasmid-mediated overexpression, thapsigargin treatment.** HCT116 cells expressing the mNeonGreen-conjugated XBP1(S) protein were reverse-transfected with either a negative control pUC19 vector or NFE2L1-expressing plasmid using the Lipofectamine LTX™ reagent. Media was substituted 6 hours prior to analysis; control media contained 0.01% DMSO (v/v) and treatment media contained 300 nM thapsigargin (Th). (A) Photomicrographs of each treatment condition (B) Graphical representation of % cells positive for fluorescent XBP1(S). The data represents mean ± S.E.M. Tukey's test analysis: *p<0.05. N=3 Scale bar 400 μm.

3.2 Flow Cytometry

3.2.1 dsRNAi-Mediated NFE2L1 Knock Down

Fluorescence of mNeonGreen-Conjugated XBP1(S) in NFE2L1 RNAi-mediated knock down conditions were quantified using flow cytometry, which corroberated the fluorescence microscopy results. Under transfected control conditions, the relative fold change in XBP1(S) fluoresence increased to 1.55±0.046-fold ($p \leq 0.01$). Under NFE2L1 knock down conditions, this fold change was reduced; treatment with thapsigargin under these conditions lead to a 1.24±0.06-fold increase in fluorescence, which was not significantly different from the knock down control ($p > 0.05$). The fold change of the knockdown sample when treated with thapsigargin was significantly lower than that of the treated control samples ($p \leq 0.05$).

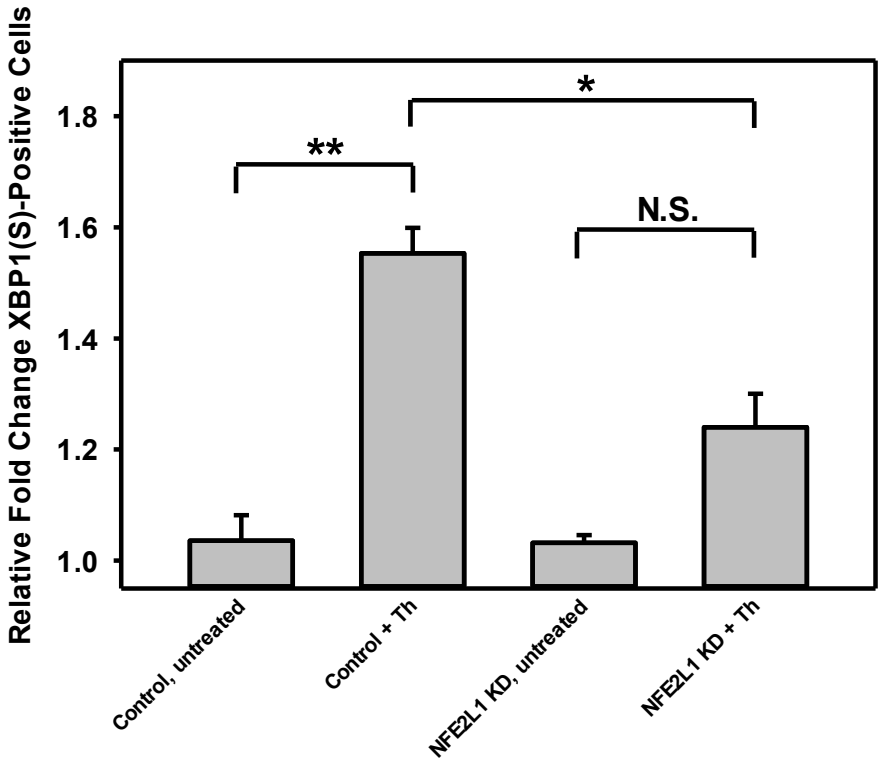

Figure 5: HCT16 cell XBP1(S)-mNeonGreen fluorescence in NFE2L1 in NFE2L1 RNAi-mediate knock down, thapsigargin treatment. HCT116 cells expressing the mNeonGreen-conjugated XBP1(S) protein were double-transfected with either a universal negative control dsRNAi oligonucleotide or NFE2L1-targeting dsRNAi oligonucleotide using the Oligofectamine reagent. Media was substituted 6 hours prior to analysis; control media contained 0.01% DMSO (v/v) and treatment media contained 300 nM thapsigargin. (A) Fluorescence vs cell count data for each treatment group (B) Graphical representation of fold change in mNeonGreen-conjugated XBP1(S) fluorescence in each treatment group. The data represents mean ± S.E.M. Tukey's test analysis: *** $p<0.001$; * $p<0.05$; N.S. non-significant. N=3. Events: 15 000.

3.2.2 Plasmid-Mediated NFE2L1 Overexpression

Fluorescence of the same cell line was likewise assessed in the context of NFE2L1 plasmid-mediated overexpression. Under transfected control conditions, the 6-hour treatment with 300 nM thapsigargin resulted in a significant increase in XBP1(S) fluorescence: a fold change of 1.88±0.12-fold ($p \leq 0.01$). However, this significant increase in fluorescence, when treated with thapsigargin, was not maintained in cells overexpressing NFE2L1 ($p > 0.05$). The fluorescence of untreated cells overexpressing NFE2L1 was significantly higher than in the transfected control, non-treated sample ($p \leq 0.05$). There was no significant difference between transfected control cells and transfected NFE2L1 overexpressing cells, when treated with thapsigargin ($p > 0.05$).

Commented [JB1]:

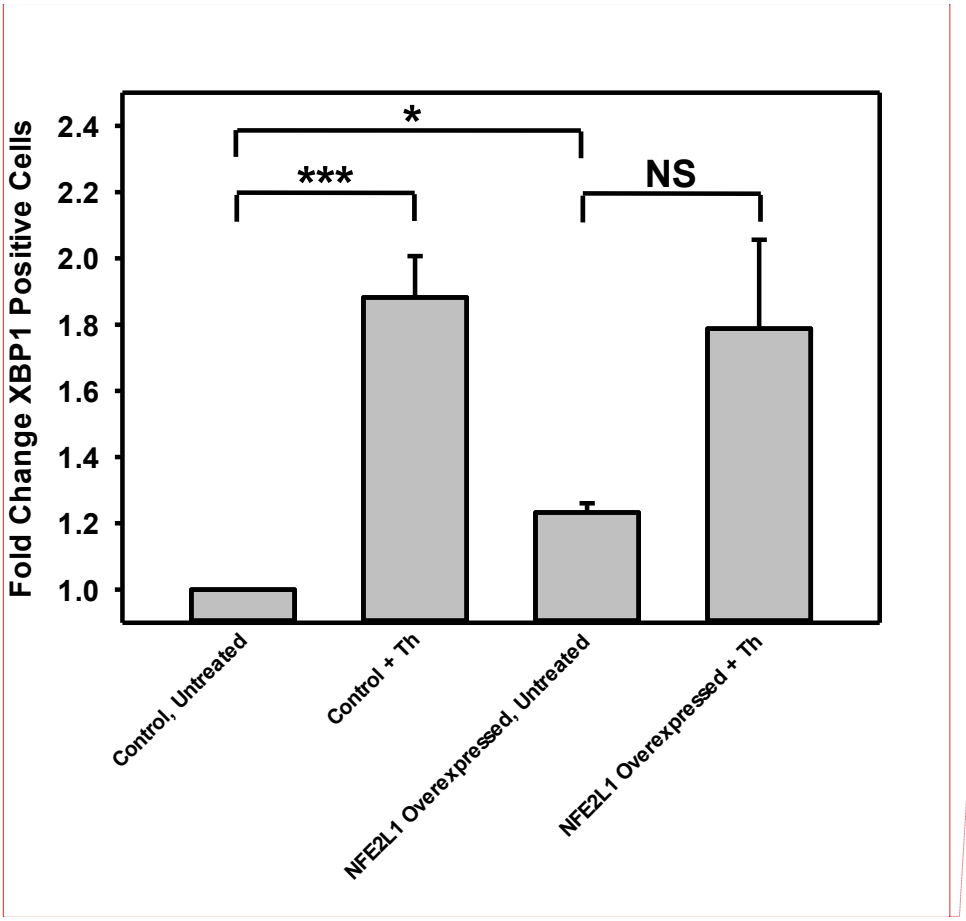

Figure 6: HCT116 cell XBP1(S)-mNeonGreen fluorescence in NFE2L1 plasmid-mediated overexpression and thapsigargin treatment. HCT116 cells expressing the mNeonGreen-conjugated XBP1(S) protein were reverse-transfected with either a pUC19 empty vector negative control or NFE2L1-expressing plasmid using the Lipofectamine LTX™ reagent. Media was substituted 6 hours prior to analysis; control media contained 0.01% DMSO (v/v) and treatment media contained 300 nM thapsigargin. (A) Fluorescence vs cell count data for each treatment group (B) Graphical representation of fold change in mNeonGreen-conjugated XBP1(S) fluorescence in each treatment group. The data represents means ± S.E.M. Tukey's test analysis: *** $p<0.001$; * $p<0.05$; N.S. non-significant. N = 3. Events: 20 000.

3.3 Western Blot

To corroborate the protein expression data derived from fluorescence microscopy and flow cytometry, the relative expression of XBP1(S) and XBP1(U) protein splice variants were analyzed by Western blot. To establish the magnitude of UPR activation in each treatment, the bands corresponding to XBP1(S) and XBP1(U) were compared, and relative quantity of the active, spliced isoform was found as a percentage of the total XBP1 expression. It was found that, when transfected with a negative control dsRNAi oligo, the percentage of XBP1 in each well increased from 41.73±2.35% to 49.91±4.92% when treated with thapsigargin. Conversely, it was found that the % expression of the spliced XBP1 isoform in conditions of NFE2L1 knock down decreased very slightly when treated with thapsigargin from 43.94±1.7% when untreated to 42.13±3.92% when treated. Overall, Western blot evidence is weaker than fluorescence data, requires further optimization, and increased sample size.

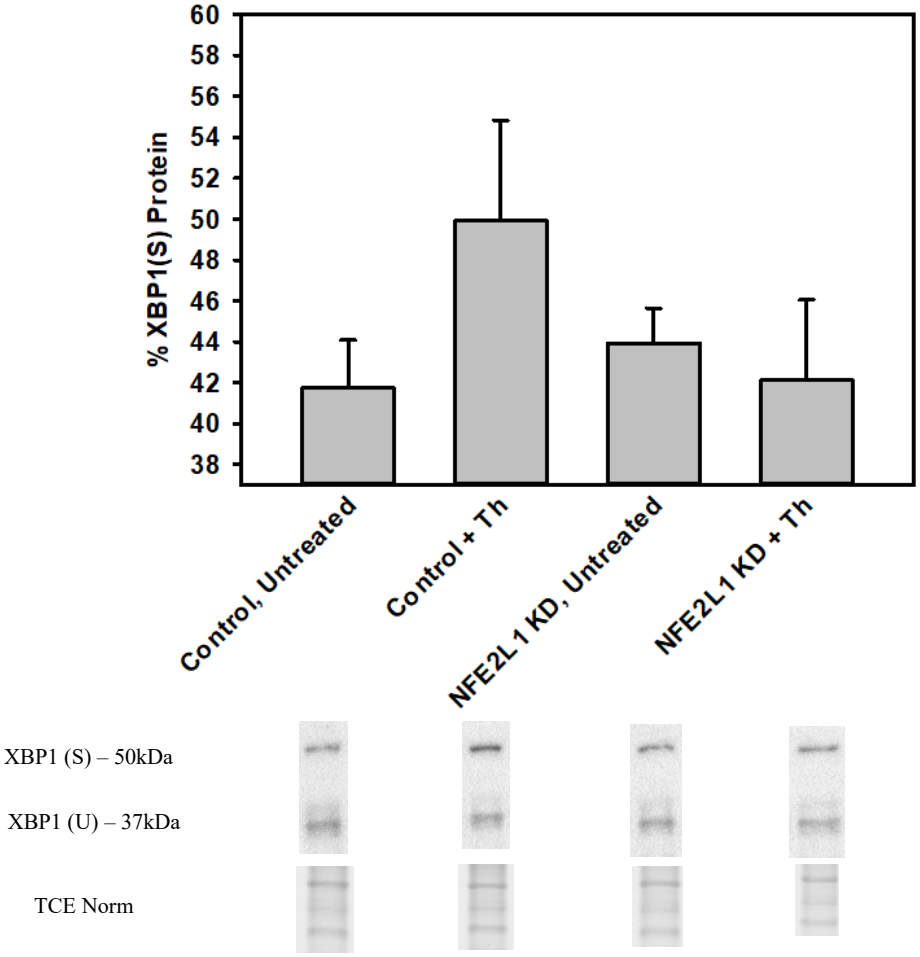

Figure 7: HCT116 cell XBP1(U+S) protein expression in RNAi-mediated knock down, thapsigargin treatment. HCT116 were double-transfected with either a negative control dsRNAi oligonucleotide or NFE2L1-targeting dsRNAi oligonucleotide using the Oligofectamine reagent. Media was substituted 6 hours prior to analysis; control media contained 0.01% DMSO (v/v) and treatment media contained 300 nM thapsigargin (Th). (A) Graphical representation of densitometry analysis of Western blot bands (B) XBP1 Western blot bands; XBP (S) at 55 kDa XBP1(U) 37 kDa. 2,2,2-trichloroethanol normalized. N=2.

3.4 RT-qPCR

To investigate whether RNAi-mediated knock down of NFE2L1 altered the splicing dynamic of XBP1 in ER stress, qPCR was performed on cDNA from cells either transfected with a negative control or NFE2L1-targeting dsRNAi oligo when either untreated or treated with 300 nM thapsigargin for 6 hours. The relative fold change in RNA expression between the transfected control cells treated with thapsigargin was of 2.26±0.037-fold, a significant increase relative to the untreated cells ($p \leq 0.01$) (Figure 8). This significant increase in RNA expression was not observed under NFE2L1 knock down conditions; XBP1(S) expression decreased slightly relative to the negative control when untreated down to 0.56±0.027-fold ($p > 0.05$) and increased significantly relative to this to 1.23±0.24-fold when treated with thapsigargin ($p \leq 0.05$). The cells treated with thapsigargin displayed a significantly greater fold change in XBP1(S) RNA relative to those with NFE2L1 knock down ($p \leq 0.05$).

The relative proportions of XBP1(S) and XBP1(U) RNA were also compared. Under transfected, negative control conditions, the proportion of XBP1(S) RNA increased from 65.13% when untreated to 84.5% when treated with 300nM thapsigargin for 6 hours. Under conditions of NFE2L1 knock down, the proportion of XBP1(S) RNA increased from 35.6% when untreated to 64.38% when treated with 300 nM thapsigargin for 6 hours (Figure 9).

When assessing the relative fold change in total XBP1 RNA in relation to XBP1(U) RNA, it is observed that total XBP1 expression triples under control conditions when treated with thapsigargin, whereas the expression of XBP1(U) increases only 1.35-fold. Under untreated NFE2L1 knock down conditions, total XBP1 and XBP1(U) expression increase 2.99-fold and 2.21-fold, respectively, relative to the negative control. Under NFE2L1 knock down and

treatment with thapsigargin, total XBP1 and XBP1(U) expression increased relative to the negative control by 2.1-fold and 2.74-fold, respectively (Figure 10).

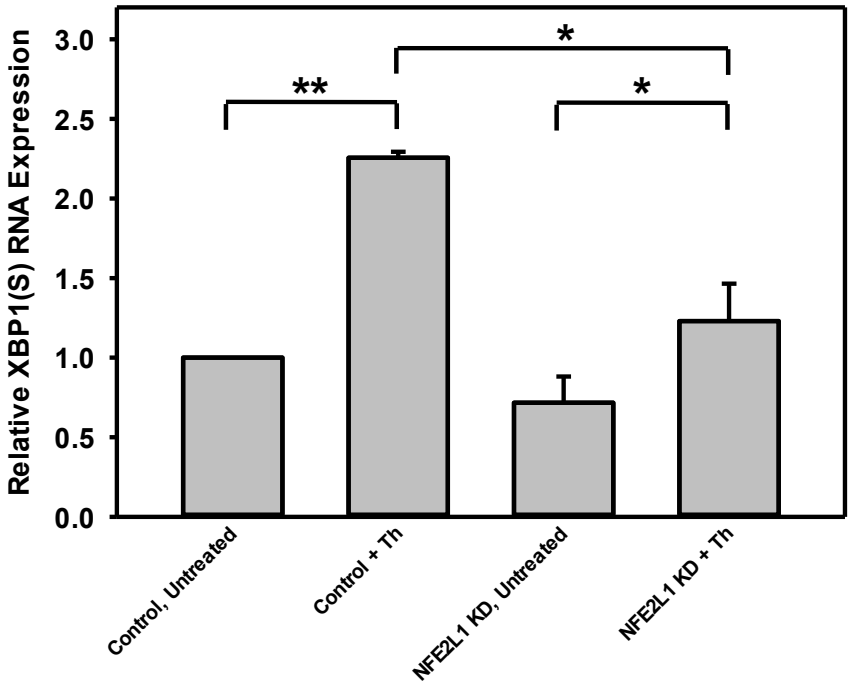

Figure 8: Relative XBP1(S) RNA expression in NFE2L1 RNAi-mediated knock down, thapsigargin treatment. HCT116 were double-transfected with either a negative control dsRNAi oligonucleotide or NFE2L1-targeting dsRNAi oligonucleotide using the Oligofectamine reagent. HCT116 were double-transfected with either a negative control dsRNAi oligonucleotide or NFE2L1-targeting dsRNAi oligonucleotide using the Oligofectamine reagent. Media was substituted 6 hours prior to analysis; control media contained 0.01% DMSO (v/v) and treatment media contained 300 nM thapsigargin. The data represents means ± S.E.M. Tukey's test analysis: ** $p<0.01$; * $P<0.05$; N.S. Non-significant) N=6.

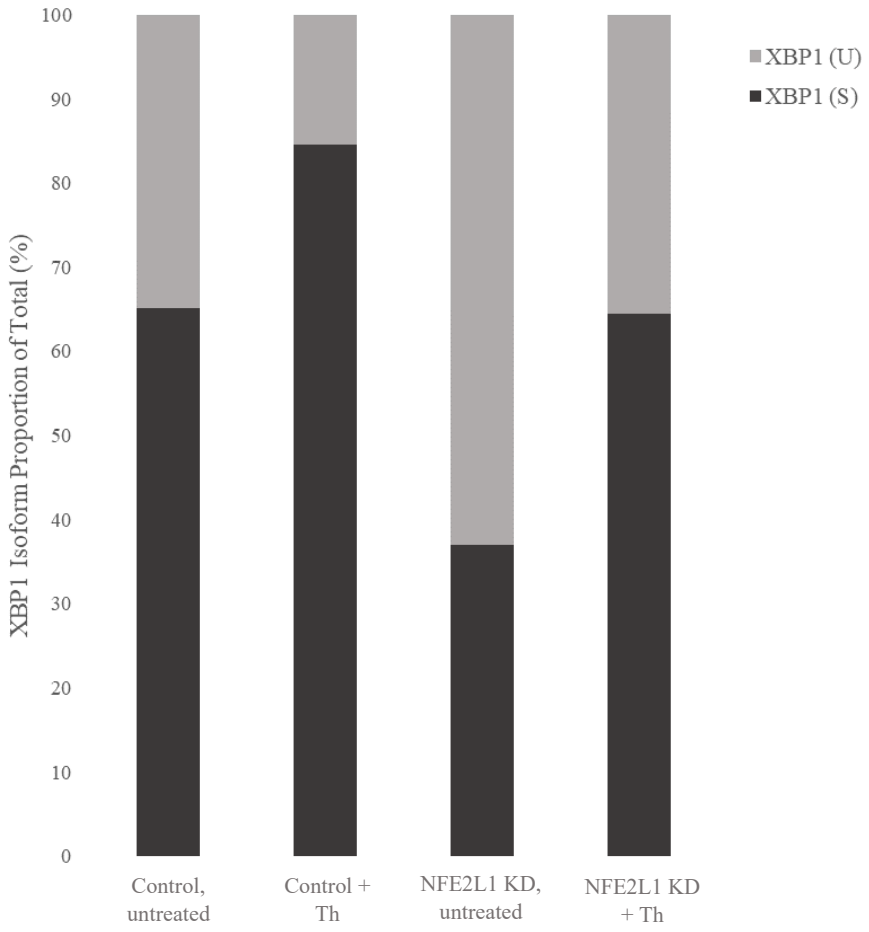

Figure 9: Percent Composition of XBP1(S) (dark grey) and XBP1(U) (light grey) RNA in NFE2L1 RNAi-mediated knock down, thapsigargin treatment. HCT116 were double-transfected with either a negative control dsRNAi oligonucleotide or NFE2L1-targeting dsRNAi oligonucleotide using the Oligofectamine reagent. Media was substituted 6 hours prior to analysis; control media contained 0.01% DMSO (v/v) and treatment media contained 300 nM thapsigargin. N=6.

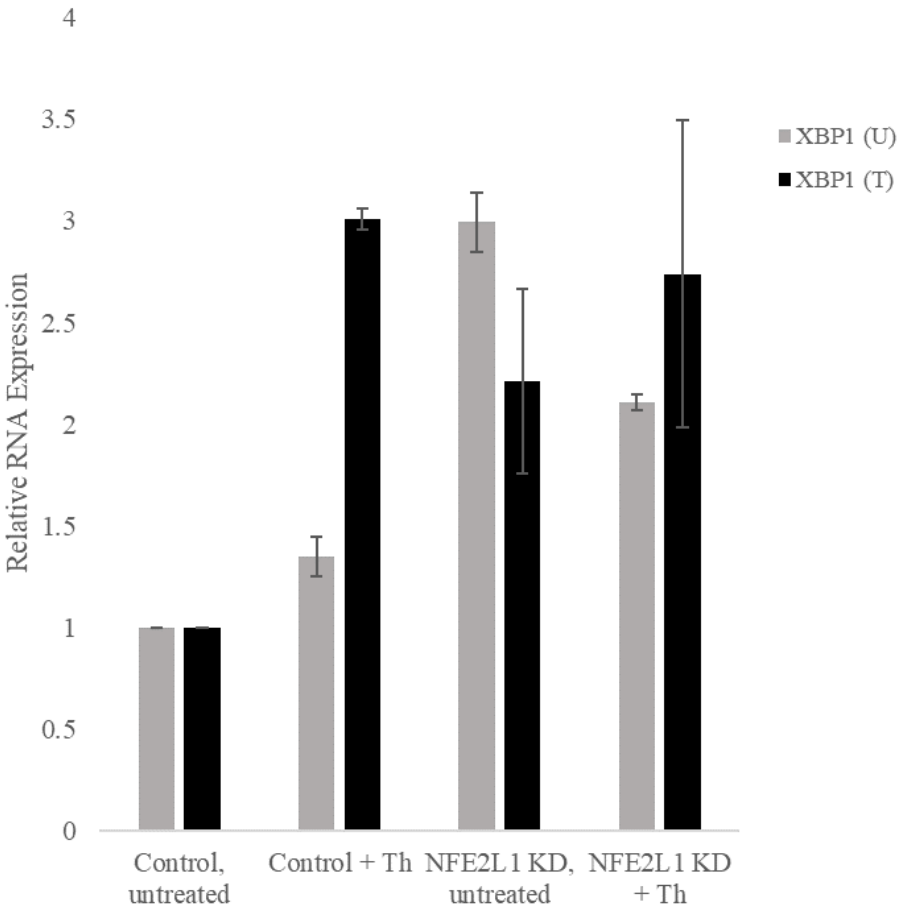

Figure 10: Relative XBP1(U) and total XBP1 RNA expression in NFE2L1 RNAi-mediated knock down, thapsigargin treatment. HCT116 were double-transfected with either a negative control dsRNAi oligonucleotide or NFE2L1-targeting dsRNAi oligonucleotide using the Oligofectamine reagent. Media was substituted 6 hours prior to analysis; control media contained 0.01% DMSO (v/v) and treatment media contained 300 nM thapsigargin. N=3.

Chapter 4: Discussion

4.1 Background

NFE2L1 is an ER-membrane-resident CNC family b-ZIP transcription factor typically associated with the antioxidant response and the synthesis of proteasomal subunits (Kim *et al*., 2016). It is released from the ER upon the cleavage of its amphipathic alpha-helical domain and is subsequently translocated to the nucleus (Kim *et al*., 2016; Dirac-Svejstrup *et al*., 2020). Once in the nucleus, NFE2L1 heterodimerizes with small Maf proteins, enhances the transcription of AREs, and regulates the production of proteasomal subunits (Kim *et al*., 2016; Zhu *et al*., 2020).

Upon ER stress elicited from the aggregation of misfolded and unfolded proteins, GRP78 dissociated from the namesake proteins of each branch of the UPR. These include ATF6, PERK, and the endonuclease IRE1α. IRE1α dimerizes, autophosphorylates, and oligomerizes into its active nuclease complex to cleave nascent XBP1 RNA. The unspliced variant of XBP1 (XBP1(U)) RNA translates a polypeptide containing a translational pause and ER localization signal. This translational pause halts XBP1(U) translation and the ER localization signal controls the translocation of the mRNA-ribosome-nascent-XBP1-polypeptide complex to the ER membrane where the endonuclease, activated IRE1α, cleaves this RNA into its spliced variant, which is translated into an active bZIP transcription factor. In the nucleus, XBP1(S) primarily enhances the transcription of many chaperone proteins and is the primary UPR effector of ERAD protein synthesis (Zhu *et* al., 2020; Yanagitani *et al*., 2011, Hetz, 2012). One such ERAD protein is the ER degradation-enhancing alpha-mannosidase protein (EDEM). EDEM is an ER lumen Class 1 alpha1,2-mannosidase family protein which enhances the degradation of misfolded

glycoproteins in the ER via extraction from the CNX-CRT cycle. This is done by cleaving mannose residues, accelerating the release of misfolded proteins detected by CNX to promote their proteasome-mediated degradation (Olivari *et al.*, 2005**).** Beyond its catalytic activity in trimming mannose residues, EDEM has also been shown to selectively bind misfolded proteins independent of the presence of glycans, and complex with downstream ubiquitin ligases to facilitate degradation (Cormier *et al*., 2009). These ubiquitin ligases, such as synoviolin, and sel-1 homolog 1 (SEL1L), are also transcriptionally regulated by XBP1 (Hwang & Li, 2018**)**. Overall, XBP1 transcriptionally involved at many levels of ERAD.

As the functions of NFE2L1 have been progressively delineated in the literature, it has been acknowledged that there exist many overlapping functions between it and the UPR. The primary similarity lies in the shared role of maintaining proteostasis. Under conditions of proteasomal inhibition, NFE2L1 is highly expressed and promotes the production of proteasomal subunits with the goal of promoting protein degradation (Kim *et al*., 2016). The UPR similarly promotes the degradation of misfolded and unfolded proteins when they aggregate. XBP1 is of particular importance to this end as it promotes several ERAD elements (Hetz, 2012). Further, the UPR reacts strongly to inhibition of the proteasome; the accumulation and aggregation of undegraded, polyubiquitinated proteins results in ER stress (Borjan *et al*., 2020). Beyond this, the activation of NFE2L1 is quite similar to many UPR effectors. In its inactive state, NFE2L1 is anchored to the ER membrane, like many UPR proteins. NFE2L1 is then cleaved, modified, and translocated to the nucleus as a b-ZIP transcription factor, like many UPR proteins (Kim *et al*., 2016; Hetz, 2012). It has also been observed that the knockout of NFE2L1 also results in ER stress. These findings, among others, appear to support the narrative that NFE2L1 may play a

role in the UPR, and as such we observed the effects of NFE2L1 overexpression and knock down on the splicing of XBP1, a crucial step in the IRE1α branch of the UPR.

To restate our hypothesis: we believe that the overexpression and knock down of NFE2L1 will alter the splicing of nascent XBP1(U) RNA into its active splice variant; specifically, we predicted that knock down will decrease the amount of XBP1(S) RNA and protein produced under ER stress conditions, and that overexpression of NFE2L1 will enhance the production of the active transcription factor variant.

Overall, the results support our hypothesis. In both protein and RNA expression, knock down of NFE2L1 reduces the amount of the active XBP1(S) variant produced, and overexpression amplified the baseline expression of the active variant protein under untreated conditions.

4.2 Discussion of Results

The relation of increased XBP1(S) expression in cells exposed to the ER stressor thapsigargin was firmly established using statistical variance analysis. Under transfected control conditions, strong statistical significance was always established; Dunnett's $p < 0.01$ - < 0.001. This is also a relationship that is well-established in the literature (Hetz *et al*., 2012). When assessing how XBP1 splicing is affected by knock down and overexpression of NFE2L1, it is in reference to this well-established relationship.

4.2.1 Fluorescence Microscopy

It was demonstrated using fluorescence microscopy and cells stably transfected to produce mNeonGreen-conjugated XBP1(S), that XBP1(S) expression decreased significantly

from the treated control cells relative to the treated cells subject to RNAi knock down of NFE2L1 ($p \leq 0.05$; Figure 3). The knock down of NFE2L1 had a negative impact on the production of XBP1(S) and by extension inhibited the adaptive response to the stressor. These results suggest that NFE2L1 facilitates the production of XBP1(S) protein. The spliced variant fusion protein demonstrates lowered expression, suggesting highly disrupted UPR signaling. Unable to reinstate proteostasis, the cell is more vulnerable to apoptosis (Hetz, 2012). If NFE2L1 is involved in the modulation of the UPR as these results suggest, reduced NFE2L1 expression could be maladaptive in some circumstances; dysfunctional UPR can lead to the uncontrollable accumulation of misfolded protein, a trademark of many disease conditions (Voisine *et al*., 2010). The relationship between NFE2L1 and the splicing dynamics of XBP1 have yet to be explored thoroughly in the literature with only one comparable experiment. The Zhang lab demonstrated by XBP1(U/S) Western blot that, in their HepG2 NFE2L1 conditional knockout cell line, XBP1(S) expression is reduced dramatically under control conditions, and expression does not achieve levels comparable to the wild type control even under ER stress conditions (Zhu *et* al, 2020). These findings are somewhat similar to what we have observed; though our results indicate that cells expressed an equally low expression of XBP1(S) when untreated, expression in treated NFE2L1 knock down cells did not show any statistically significant change (Figure 3) At the level of protein analysis, it cannot be determined from ours or the Zhang lab results the level at which NFE2L1 could modulate the splicing of XBP1; i.e. at the level of transcription (ex. promoter/enhancer-binding) or mRNA processing (interaction with IRE1α), or otherwise.

Overexpression of NFE2L1 in the cells expressing the mNeonGreen-XBP1(S) fusion protein resulted in a significant increase in the baseline XBP1(S) positivity in untreated cells ($p \leq$

0.05; Figure 4); the moderate statistical significance of these results is the result of an outlier in the overexpressed control cells with 50% the positivity of the other samples; with replication, I am confident the statistical significance can be strengthened. Nonetheless, these results further support the argument that NFE2L1 is involved in the production of XBP1 protein. Increasing the baseline expression of the spliced isoform strengthens the UPR; overexpression of XBP1 has been demonstrated as protective in misfolded protein pathologies. In a Parkinson's disease model, XBP1(S) overexpression was neuroprotective, compensating even for treatment with the proteasome inhibitor 1-methyl-4-phenylpyridinium (Sado, 2009). However, the pro-survival signaling of XBP1(S) has also been observed in cancer, enabling it to thrive in the tumour microenvironment with heightened metabolic activity. Further, XBP1(S) overexpression in cancer is correlated with poor clinical outcomes, and increased chemoresistance (Wu *et* al., 2018). Thus, enhancing the UPR can be both advantageous and deleterious depending on the disease, and the apparent involvement of NFE2L1 in its activity, as our evidence suggests, may prove an effective, indirect avenue for modulating its expression prior to its activation.

The increase in XBP1(S) positivity in NFE2L1-overexpressing cells under thapsigargin treatment was statistically significant ($p \leq 0.05$). However, the level of XBP1(S) fusion protein fluorescence positivity did not increase significantly between the treated transfected control cells and those treated overexpressing NFE2L1 ($p > 0.05$). Though positivity was increased by 60% in the overexpressing cells, high variance in the overexpressing samples resulted in a lack of statistical significance; it will be interesting to see if statistical significance can be achieved through increase in replication. There may also be another factor influencing this relationship: it is acknowledged in the publication that established the protocol to generate the stably transfected cell line that, even under positive control conditions where all cells should theoretically

fluoresce, not all cells display positivity (Nougarède *et al*., 2018). The reporter in question is imperfect as many cells do not carry the vector to produce the XBP1-mNeonGreen fusion protein, displaying a false negative under conditions of predictably high XBP1(S) expression. As a result, it is difficult to assess the difference between the NFE2L1 overexpressing and control cells when treated with thapsigargin as both may achieve the maximum induction of XBP1(S)-positive cells possible with this vector. Nonetheless, repetitions will be performed with the best cell stocks to investigate further if a statistically significant relation can be asserted. Referring again to the paper by Zhu and colleagues, indirect and modest NFE2L1 overexpression was achieved by overexpressing NFE2L2, another CNC bZIP transfection factor and master-regulator of the antioxidant response (2020). By doing this, they observed (by Western blot) a moderate increase in expression of GRP78, the primary regulator of the UPR, but not of XBP1(S) under ER stress conditions. However, the overexpression was indirect, and the ER stressor chosen was tunicamycin, which inhibits glycosylation in the ER – a process necessary for the activation and nuclear translocation of NFE2L1 (Kim *et al*., 2016). Our experimental design circumvents the inhibitory effect of tunicamycin on NFE2L1 activation by inducing ER stress using thapsigargin, which has no direct effect on glycosylation, and by overexpressing NFE2L1 directly by plasmid transfection. It has recently been shown that NFE2L1 may bind an ARE in the promoter region of XBP1. This suggests a possible link between NFE2L1 and XBP1 expression under ER stress conditions, which could explain the increased baseline XBP1 under NFE2L1 overexpresion (Zhu *et al*., 2020).

4.2.2 Flow Cytometry

Flow cytometry was used to increase the population of cells counted relative to fluorescence microscopy, and to eliminate unconscious personal bias in cell counts and determination of XBP1(S) fluorescence. These results largely corroborated the findings of individual cell counts in fluorescence microscopy. RNAi knock down of NFE2L1 resulted in a decreased fold change between untreated and treated cells to the extent of eliminating any statistically significant difference between the samples. This is in contrast to the strongly significant increase in fluorescence between treated and untreated cells under transfected control conditions ($p \leq 0.01$). Further, it was established that XBP1(S) fluorescence fold change was significantly higher under treated transfected control cells than those treated under NFE2L1 knock down conditions ($p \leq 0.05$). To reiterate what is known in the literature, the only comparable experiment was that performed by Zhu and colleagues where the NFE2L1 conditional knockout cells demonstrated a decrease in XBP1(S) when untreated, and did not surpass the expression shown in the untreated cells even when treated with thapsigargin. Though the cells in which NFE2L1 were knocked down did not demonstrate reduced XBP1(S) fluorescence when untreated, XBP1(S) fluorescnce did not significantly exceed that observed in the control sample when exposure to the ER stressor thapsigargin. Thus, these data corroborate the disruption in the production of XBP1(S) under NFE2L1 knock down conditions observed with fluorescence microscopy, suggesting a possible role in the UPR.

Flow cytomtetry results analyzing XBP1(S) fluorescence under conditions of NFE2L1 overexpression also corroborate fluorescence microscopy results. XBP1(S) fluorescence was significantly higher in untreated cells overexpressing NFE2L1 than in transfected control, untreated cells ($p \leq 0.05$). However, statistical significance was not found between treated and untreated NFE2L1-overexpressing cells ($p > 0.05$). Though the mean fold change demonstrated

an increase in fluorescence, the lack of statistical significance may be attributable to very high variance in this sample group, meaning that more replications will need to be performed to increase confidence in these findings. Thereover, an increase in fluorescence in treated cells under NFE2L1 overexpression conditions was not observed relative to the cells treated under normal conditions. This may be related to the previously described plateau in the number of cells that can exhibit fluorescence with the reporter as described above. Nonetheless, more assays must be performed to assess whether this remains consistent.

Overall, using the HCT116 expressing the mNeonGreen-conjugated XBP1(S), we were able to establish a disruption in the production of the spliced, active isoform when treated with thapsigargin when NFE2L1 is knocked down, and a higher expression of this isoform under untreated conditions when NFE2L1 is overexpressed. These provide important preliminary evidence for the involvement of NFE2L1 in the IRE1α branch of the UPR. Once more, the only comparable experiment in the literature was that performed by Zhu and colleagues which demonstrated a decreased expression of XBP1(S) in a NFE2L1 conditional knockout cell line when untreated, and that XBP1(S) activation under ER stress conditions was reduced compared to the control.

4.2.3 Western Blotting

The proportion of spliced XBP1 protein was calculated from the intensity of the band corresponding to the spliced isoform over the combined intensity of the bands from both isoforms. The intensities were normalized by TCE stain-free imaging of the total protein of each band and normalizing to the control. As expected, the % XBP1(S) increased under control

conditions when treated with thapsigargin. Under NFE2L1 dsiRNA-mediated knock down, however, this increase was not observed between the untreated and treated samples. This suggests that NFE2L1 is important in the production of the spliced, active transcription factor variant of this important ERAD effector. Using this method, it is also possible to assess the quantity of XBP1(U) protein under NFE2L1 knock down conditions. The intensity of the band corresponding to XBP1(U) does not appear to change under knock down conditions, suggesting NFE2L1 knock down may affect the overall protein expression of XBP1 as well as the synthesis of the active isoform. As previously stated, NFE2L1 may mediate XBP1 expression by binding to its ARE, through this requires further investigation.

4.2.4 Cell viability

It was also observed that NFE2L1 knock down resulted in decreased cell viability under ER stress conditions. The double transfection protocol is quite harsh on the cells, particularly when two reverse transfections were performed as part of optimization. However, though all untreated cells exhibited similar viability, it was noted that treatment with thapsigargin differentiated the control from the NFE2L1 knock down cells (unpublished results). Cell viability of NFE2L1-knock down cells treated with thapsigargin was so low that it was quite difficult to find large enough sample sizes of live cells on one micrograph to count during the optimization of the transfection protocol, even after optimization. One explanation may be that the co-treatment resulted in excessive stress, resulting in apoptotic signaling. Another explanation for this phenomenon lies in the role of NFE2L1 in the synthesis of proteasomal subunits. When NFE2L1 is knocked down, so to is the cell's ability to degrade protein

aggregates, and thus apoptotic signaling is initiated (Waku *et* al., 2020). Another possible reason for this lies in the role of NFE2L1 in regulating synoviolin, an E3 ER-membrane-resident ubiquitin ligase which targets IRE1α for ubiquitination and degradation in an ER-stress-dependent manor. The synoviolin promoter region, through which NFE2L1 regulates synoviolin is shared with XBP1 and normally serves as a UPR negative feedback loop with the goal of reducing downstream UPR pro-apoptotic signaling. In the literature, NFE2L1 knock down has been shown to decreased expression of synoviolin, resulting in reduced cell viability under ER stress conditions (Li *et al*., 2015) Thus, NFE2L1 expression is essential in survival under ER stress conditions.

4.2.5 RT-qPCR

RT-qPCR was performed to establish the relationship between the spliced (active) and unspliced isoforms of XBP1 when treated with thapsigargin in both control conditions and when NFE2L1 is knocked down by RNA interference. It was observed that, under transfected control conditions, XBP1(S) RNA expression increases significantly when exposed to thapsigargin ($p \leq 0.01$). A statistically significant increase in XBP1(S) expression was also observed between untreated and treated samples under conditions of NFE2L1 knock down, though this was the result of the reduced baseline expression of XBP1(S) when untreated. The treated knock down cells showed no statistical increase in expression relative to the untreated control ($p > 0.05$). These results suggest that the NFE2L1 knock down has altered the cell's ability to produce the active spliced variant of XBP1. In the literature, the only comparable experiment was performed in the same paper by Zhu and colleagues. The NFE2L1 knockout HepG2 cells were treated with

tunicamycin, and XBP1 mRNA expression increased significantly. However, it must be noted that the primers used to assert this measured only total XBP1; the proportions of each isoform were not considered. Our results demonstrate that there was indeed an increase in overall XBP1 mRNA expression when treated with an ER stressor, but it was predominantly in the spliced isoform. This can be observed more clearly when analyzing the proportions of each isoform. Under transfected control conditions, the percentage of XBP1(S) expressed in the cell increases from 65.1% to 84.5% when the thapsigargin treatment is applied. Conversely, under NFE2L1 knock down conditions, the percentage of XBP1(S) expressed is much lower at 35.6% and increases to 64.4% under thapsigargin treatment – proportions comparable to the untreated control sample. Given the above results, NFE2L1 knock down has the effect of both reducing the amount of XBP1(S) RNA under control conditions, and negatively impacting the cell's ability to splice nascent XPB1 RNA under conditions of ER stress. This observation resolves the uncertainty regarding the source of the reduced fluorescence of the XBP1(S)-mNeonGreen reporter and reduced XBP1(S) band intensity in Western blot under knock down conditions – regulation takes place at the level of RNA splicing. Further, when comparing the magnitude of fold change in the RNA expression of total XBP1 and that of XBP1(U) under control and NFE2L1 knock down conditions, discrepancies were observed. Under control conditions, treatment with thapsigargin induces a 3-fold change in the expression of total XBP1, whereas XBP1 (U) expression only increases by 1.35-fold. Under NFE2L1 knock down conditions, untreated cells exhibit a 3-fold increase in XBP1(U) expression compared to the untreated control, suggesting the accumulation of the unspliced isoform. This fold change exceeds that of the total XBP1, which is likely driven primarily by this XBP1(U) accumulation. When treated with thapsigargin, NFE2L1-knock down cells exhibit a 2.74-fold increase in total XBP1

expression compared to the untreated control, but the fold change in XBP1(U) related to thapsigargin treatment increases 2-fold, suggesting a much more substantial contribution to the total XBP1 fold change. This increased XBP1(U) fold change, in addition to the unchanged total XBP1 fold change exhibited by both treatment groups, suggests that NFE2L1 knock down cells demonstrate an inhibited capacity for splicing nascent XBP1 mRNA into that which translated into the active transcription factor. This evidence suggests that NFE2L1 may play a role in the splicing of XBP1 RNA, leading to the decreased production of the active protein isoform as observed in Western blot and reduced XBP1(S)-mNeonGreen fusion protein. Thus, the prior ambiguity regarding the level of regulation of XBP1 appears resolved; the expression of total XBP1 RNA is not altered under NFE2L1 knock down, but the splicing of its RNA is altered. The nature of this interaction requires analysis; the structure and topology of NFE2L1 has been studied extensively, and it is certainly not directly involved with the splicing of XBP1 as it does not possess a nuclease domain (Kim *et al*., 2016).

4.3 Limitations

It must be emphasized, however, that though these results are exciting, they are still preliminary. This study is limited primarily in how it defines the role of NFE2L1 in the UPR. Though the results indicate some involvement, no protein interactions were explicitly explored to explain the phenomenon. Establishing such interactions would require co-immunoprecipitation and yeast two-hybrid experiments. Although the precise structure of NFE2L1 has not yet been analyzed by X-ray crystallography or NMR, the domains of NFE2L1 protein have been studied quite extensively. There is currently no support for the notion that NFE2L1 and IRE1α could

interact directly in the ER membrane to facilitate the splicing of XBP1 RNA, and thus the nature of its involvement is likely indirect, complicating the study of this relationship (Kim *et al*., 2016). Further, the scale of the results should be increased to reduce the variance in results and increase the statistical significance of this relationship and consequently the already low probability of false positivity. Additionally, the number of assays should be increased. Though I have confidence in the data disseminated from HCT116 cells expressing mNeonGreen-conjugated XBP1(S) protein, not all cells express the fusion protein (as described in the publication from which the protocol was derived) (Nougarède *et al*., 2018). This is likely the reason that, under positive control conditions where the cells are treated for the optimal amount of time with a high concentration of thapsigargin, the cells do not show 100% positivity. Further, this may explain why the NFE2L1-overexpressing cells treated with thapsigargin did not show statistically significant increase XBP1(S)-mNeonGreen positivity – there may be a maximal number of cells that can possess the reporter to fluoresce under treatment, resulting in a plateau of XBP1(S)-mNeonGreen positivity. With the additional complication of the poor reproducibility of Western blotting, there is a need to include more protein assays to increase the confidence in the effect of NFE2L1 on XBP1 splicing at the level of protein. We will be testing for AREs in the promoters of XBP1 splicing factors, including IRE1α. When discussing increasing the variability in assays investigating protein expression, it is important to acknowledge that the genomic results of this thesis are contingent upon a single assay: RT-qPCR. To increase confidence in the genomic relation between NFE2L1 and XBP1 splicing, a greater diversity of experiments will need to be performed. Further diversification could also arise from assessing this relationship in different cell lines. These experiments were performed in human colorectal cancer cell lines, and thus it would be interesting to assess whether the role of

NFE2L1 has as influential a role in a non-cancerous equivalent cell line such as in HIEC (human intestinal crypt cells). In line with diversifying cell lines, it would be interesting to establish a knockout cell line of NFE2L1 and observe the UPR in those circumstances, since a 100% knockout of NFE2L1 RNA is not possible with conventional RNAi. Our lab had attempted in CRISPR-Cas9 knockout in HEK293T cells (Human Embryonic Kidney cells), but this was unsuccessful as it caused lethality. The Zhang lab, however, has been successful in establishing a conditional NFE2L1 knockout cell line (Zhu *et al*., 2020).

4.4 Implications of Results

Though these results are still very preliminary, they provide interesting insight in support of the involvement of NFE2L1 in the modulation of the UPR. It has been demonstrated that manipulation of NFE2L1 expression by knock down and overexpression, the dynamics of XBP1 splicing are altered; the null hypothesis that the expression pattern of XBP1 would be unchanged under such circumstances can thus be rejected.

These results are significant because they offer greater insight into the modulation of the UPR, an essential process in maintaining cell proteostasis. If more evidence is collected to confirm the relation between NFE2L1 and the splicing of XBP1, then the modulation of NFE2L1 expression may be a useful target for therapeutics seeking to modulate the UPR. If the goal is to amplify the UPR, for example, it is much easier to modulate the expression of NFE2L1 than it would be to control the proportion of XBP1 that is spliced into the active isoform. Further, there is evidence to suggest that NFE2L1 expression may affect other branches of the UPR, and thus it would prove an easier target than seeking to modulate every branch individually (Zhu, 2020).

For example, it has been suggested that, when NFE2L1 is overexpressed and contributing to the progression of cancer in response to common proteasome-inhibition chemotherapeutics, the protease DDI2 should targeted. As previously mentioned, this cleaves NFE2L1 for its release from the ER membrane for its translocation to then nucleus. An inhibitor of DDI2 would reduce the adaptive response of cancer cells to increase the production of proteasomal subunits via NFE2L1 and, if a link is established between it and the UPR, may have the indirect effect of inhibiting its pro-survival signaling (Dirac-Svejstrup *et al*., 2020).

4.3.1 UPR Function and Disease

These preliminary pieces of evidence are important in expanding our understanding of how the UPR functions. The UPR is essential in maintaining homeostasis in the ER, an organelle that serves several important functions within the cell. Of primary importance is the protein folding capacity of the cell; one third of all proteins are at least partially processed by the ER, and maintaining ideal conditions to enable this processing is of paramount importance. Prolonged ER stress has been implicated in a great variety of diseases associated with numerous organ systems. The aggregation of misfolded proteins is a hallmark of neurodegenerative diseases such as Alzheimers', Parkinson's and Amyotrophic Lateral Sclerosis (Ghemrawi & Khair, 2020). The proteotoxicity of misfolded protein aggregates can be resolved only by the UPR; prolonged, unresolved ER stress results in cell death. UPR protein expression has been strongly correlated with the onset and progression of neurodegenerative diseases (Scheper & Hoozemans, 2015). A compromised UPR could prove a risk factor for neurodegenerative diseases, and artificially amplifying the UPR may prove an innovative therapeutic (Remondelli

& Renna, 2017). XBP1 overexpression specifically has been shown to be neuroprotective in Parkinson's disease models (Valdés *et al*., 2014, Sado *et al*., 2009). If NFE2L1 expression is implicated in the UPR as our evidence suggests, then it may present an interesting therapeutic target, and its downregulation a possible risk factor.

4.3.1.1 Cancer

In cancer, UPR signalling mechanisms enhance the cancer cell's survival in the harsh tumor microenvironment, and limit the effectiveness of conventional therapies. Many of the stressors that cancer cells produce in their tumor microenvironment also trigger the adaptive UPR: hypoxia, oxidative stress, acidosis, nutrient deficiency, cytotoxicity, etc. (Moenner *et al*., 2007). Cancer progression and metastasis are also strongly correlated with elevated expression of UPR proteins, and treatment with chemotherapeutics further exacerbate this overexpression (Wang *et al*., 2019; Xie *et al*., 2016). In a chemoresistant breast cancer cell line, RNAi-mediated knock down of GRP78 was shown to reduce cell viability when treated with gemcitabine. Overexpression of GRP78 had the opposite effect (Xie *et al*., 2016). By targeting UPR proteins, such therapeutics aim to diminish the cell's defenses to overcome the survival mechanisms that make cancer such a complicated disease to treat. By understanding more about the UPR, such as the possible involvement of NFE2L1, we can envisage the development of more sophisticated therapeutics, and help predict the possible compensatory mechanisms that hinder the effectiveness of such therapeutics.

4.4 Concluding Remarks

In conclusion, we have found preliminary evidence that suggests that NFE2L1 may be implicated in the UPR in HCT116 cells. It was demonstrated that, at both the level of protein and RNA, the production of the spliced form of XBP1 was stunted under RNAi-mediated NFE2L1 knock down conditions when treated with thapsigargin. Further, the baseline level of spliced XBP1 protein increased significantly when NFE2L1 was overexpressed. These findings strongly suggest that NFE2L1 is involved in some capacity in the splicing of XBP1 into its active UPR effector. If this relationship can be reaffirmed through repetition, greater diversity of assays, and the delineation of the specific interactions between NFE2L1 and the UPR, it could prove an important finding in developing our understanding of this stress response. This would present a new avenue by which to explore the potential of therapeutics targeted to the UPR. Since the UPR is an important pro-survival function in cancers, for example, reducing this defense through modulation of NFE2L1 may render cancers more chemo sensitive.

Chapter 5: References

Adams, B. M., Oster, M. E., & Hebert, D. N. (2019). Protein quality control in the endoplasmic reticulum. *Protein Journal*, ***38***(3), 317–329. https://doi.org/10.1007/s10930-019-09831-w

Bartelt, A., Widenmaier, S. B., Schlein, C., Johann, K., Goncalves, R. L. S., Eguchi, K., … Hotamisligil, G. S. (2018). Brown adipose tissue thermogenic adaptation requires Nrf1-mediated proteasomal activity. *Nature Medicine*, ***24***(3), 292–303. https://doi.org/10.1038/nm.4481

Berridge, M. J. (2002). The endoplasmic reticulum: A multifunctional signaling organelle. *Cell Calcium*, ***32***(5–6), 235–249. https://doi.org/10.1016/S0143416002001823

Bian, T., Autry, J. M., Casemore, D., Li, J., Thomas, D. D., He, G., & Xing, C. (2016). Direct detection of SERCA calcium transport and small-molecule inhibition in giant unilamellar vesicles. *Biochemical and Biophysical Research Communications*, ***481***(3–4), 206–211. https://doi.org/10.1016/j.bbrc.2016.10.096

Borjan, B., Kern, J., Steiner, N., Gunsilius, E., Wolf, D., & Untergasser, G. (2020). Spliced XBP1 levels determine sensitivity of multiple myeloma cells to proteasome inhibitor Bortezomib independent of the unfolded protein response mediator GRP78. *Frontiers in Oncology*, ***9***, 1–11. https://doi.org/10.3389/fonc.2019.01530

Braakman, I., & Bulleid, N. J. (2011). Protein folding and modification in the mammalian endoplasmic reticulum. *Annual Review of Biochemistry*, ***80***, 71–99. https://doi.org/10.1146/annurev-biochem-062209-093836

Brehme, M., Sverchkova, A., & Voisine, C. (2019). Proteostasis network deregulation signatures as biomarkers for pharmacological disease intervention. *Current Opinion in Systems Biology*, ***15***, 74–81. https://doi.org/10.1016/j.coisb.2019.03.008

Bugno, M., Daniel, M., Chepelev, N. L., & Willmore, W. G. (2015). Changing gears in Nrf1 research, from mechanisms of regulation to its role in disease and prevention. *Biochimica et Biophysica Acta - Gene Regulatory Mechanisms*, ***1849***(10), 1260–1276. https://doi.org/10.1016/j.bbagrm.2015.08.001

Caramelo, J. J., & Parodi, A. J. (2008). Getting in and out from calnexin/calreticulin cycles. *Journal of Biological Chemistry*, ***283***(16), 10221–10225. https://doi.org/10.1074/jbc.R700048200

Chen, C. -y., Malchus, N. S., Hehn, B., Stelzer, W., Avci, D., Langosch, D., & Lemberg, M. K. (2014). Signal peptide peptidase functions in ERAD to cleave the unfolded protein response regulator XBP1u. *The EMBO Journal*, ***33***(21), 2492–2506. https://doi.org/10.15252/embj.201488208

Chen, H. ying, Ren, X. yan, Wang, W. hua, Zhang, Y. xin, Chen, S. feng, Zhang, B., & Wang, L. xin. (2014). Upregulated ROS production induced by the proteasome inhibitor MG-132 on XBP1 gene expression and cell apoptosis in Tca-8113 cells. *Biomedicine and Pharmacotherapy*, ***68***(6), 709–713. https://doi.org/10.1016/j.biopha.2014.07.011

Chevillard, G., & Blank, V. (2011). NFE2L3 (NRF3): The Cinderella of the Cap'n'Collar transcription factors. *Cellular and Molecular Life Sciences*, ***68***(20), 3337–3348. https://doi.org/10.1007/s00018-011-0747-x

Cormier, J. H., Tamura, T., Sunryd, J. C., & Hebert, D. N. (2009). EDEM1 recognition and delivery of misfolded proteins to the SEL1L-containing ERAD complex. Molecular Cell, ***34***(5), 627–633. https://doi.org/10.1016/j.molcel.2009.05.018.EDEM1

Crompton, M., Costi, A., & Hayat, L. (1987). Evidence for the presence of a reversible Ca2+-dependent pore activated by oxidative stress in heart mitochondria. *The Biochemical Journal*, ***245***(3), 915–918. https://doi.org/10.1042/bj2450915

Cui, Q., Fu, J., Hu, Y., Li, Y., Yang, B., Li, L., … Pi, J. (2017). Deficiency of long isoforms of Nfe2l1 sensitizes MIN6 pancreatic β cells to arsenite-induced cytotoxicity. *Toxicology and Applied Pharmacology*, ***329***, 67–74. https://doi.org/10.1016/j.taap.2017.05.013

Digaleh, H., Kiaei, M., & Khodagholi, F. (2013). Nrf2 and Nrf1 signaling and ER stress crosstalk: Implication for proteasomal degradation and autophagy. *Cellular and Molecular Life Sciences*, ***70***(24), 4681–4694. https://doi.org/10.1007/s00018-013-1409-y

Dirac-Svejstrup, A. B., Walker, J., Faull, P., Encheva, V., Akimov, V., Puglia, M., … Svejstrup, J. Q. (2020). DDI2 is a ubiquitin-directed endoprotease responsible for cleavage of transcription factor NRF1. *Molecular Cell*, ***79***(2), 332-341.e7. https://doi.org/10.1016/j.molcel.2020.05.035

Dodson, M., De La Vega, M. R., Cholanians, A. B., Schmidlin, C. J., Chapman, E., & Zhang, D. D. (2019). Modulating NRF2 in disease: Timing is everything. *Annual Review of Pharmacology and Toxicology*, ***59***, 555–575. https://doi.org/10.1146/annurev-pharmtox-010818-021856

Duran-Aniotz, C., Cornejo, V. H., Espinoza, S., Ardiles, Á. O., Medinas, D. B., Salazar, C., … Hetz, C. (2017). IRE1 signaling exacerbates Alzheimer's disease pathogenesis. *Acta Neuropathologica*, ***134***(3), 489–506. https://doi.org/10.1007/s00401-017-1694-x

Ellgaard, L., & Helenius, A. (2001). ER quality control: towards an understanding at the molecular level. *Cell Biology* ***13***. 431-437.

Ellgaard, L., & Helenius, A. (2003). Quality control in the endoplasmic reticulum. Nature Reviews Molecular Cell Biology, ***4***(3), 181–191. https://doi.org/10.1038/nrm1052

Ellgaard, L., McCaul, N., Chatsisvili, A., & Braakman, I. (2016). Co- and Post-Translational Protein Folding in the ER. *Traffic*, ***17***(6), 615–638. https://doi.org/10.1111/tra.12392

Erfle, H., Neumann, B., Liebel, U., Rogers, P., Held, M., Walter, T., … Pepperkok, R. (2007). Reverse transfection on cell arrays for high content screening microscopy. Nature Protocols, ***2***(2), 392–399. https://doi.org/10.1038/nprot.2006.483

Gao, H. J., Zhu, Y. M., He, W. H., Liu, A. X., Dong, M. Y., Jin, M., … Huang, H. F. (2012). Endoplasmic reticulum stress induced by oxidative stress in decidual cells: A possible mechanism of early pregnancy loss. *Molecular Biology Reports*, ***39***(9), 9179–9186. https://doi.org/10.1007/s11033-012-1790-x

Ghemrawi, R., & Khair, M. (2020). Endoplasmic reticulum stress and unfolded protein response in neurodegenerative diseases. *International Journal of Molecular Sciences*, ***21***(17), 1–25. https://doi.org/10.3390/ijms21176127

Gidalevitz, T., Stevens, F., & Argon, Y. (2013). Orchestration of secretory protein folding by ER chaperones. Biochimica et Biophysica Acta - Molecular Cell Research, ***1833***(11), 2410–2424. https://doi.org/10.1016/j.bbamcr.2013.03.007

Gonzalez-Donquiles, C., Alonso-Molero, J., Fernandez-Villa, T., Vilorio-Marques, L., Molina, A. J., & Martin, V. (2017). The NRF2 transcription factor plays a dual role in colorectal cancer: A systematic review. *PLoS ONE*, ***12***(5), 1–14. https://doi.org/10.1371/journal.pone.0177549

Graner, M. W., Lillehei, K. O., & Katsanis, E. (2015). Endoplasmic Reticulum Chaperones and Their Roles in the Immunogenicity of Cancer Vaccines. Frontiers in Oncology, ***4***(January), 1–12. https://doi.org/10.3389/fonc.2014.00379

Guna, A., & Hegde, R. S. (2018). Transmembrane domain recognition during membrane protein biogenesis and quality control. *Current Biology*, ***28***(8), R498–R511. https://doi.org/10.1016/j.cub.2018.02.004

Guo, F. J., Lin, E. A., Liu, P., Lin, J., & Liu, C. (2010). XBP1U inhibits the XBP1S-mediated upregulation of the iNOS gene expression in mammalian ER stress response. *Cellular Signalling*, ***22***(12), 1818–1828. https://doi.org/10.1016/j.cellsig.2010.07.006

Han, W., Ming, M., Zhao, R., Pi, J., Wu, C., & He, Y. Y. (2012). Nrf1 CNC-bZIP protein promotes cell survival and nucleotide excision repair through maintaining glutathione homeostasis. *Journal of Biological Chemistry*, ***287***(22), 18788–18795. https://doi.org/10.1074/jbc.M112.363614

Hao, L., Zhong, W., Dong, H., Guo, W., Sun, X., Zhang, W., … Zhou, Z. (2020). ATF4 activation promotes hepatic mitochondrial dysfunction by repressing NRF1-TFAM signalling in alcoholic steatohepatitis. *Gut*, ***0***, 1–13. https://doi.org/10.1136/gutjnl-2020-321548

He, Y., Sun, S., Sha, H., Liu, Z., Yang, L., Xue, Z., … Qi, L. (2010). Emerging roles for XBP1, a sUPeR transcription factor. *Gene Expression*, ***15***(1), 13–25. https://doi.org/10.3727/105221610X12819686555051

Hetz, C. (2012). The unfolded protein response: Controlling cell fate decisions under ER stress and beyond. *Nature Reviews Molecular Cell Biology*, ***13***(2), 89–102. https://doi.org/10.1038/nrm3270

High, S., Lecomte, F. J. L., Russell, S. J., Abell, B. M., & Oliver, J. D. (2000). Glycoprotein folding in the endoplasmic reticulum: A tale of three chaperones? *FEBS Letters*, ***476***(1–2), 38–41. https://doi.org/10.1016/S0014-5793(00)01666-5

Hinte, F., Van Anken, E., Tirosh, B., & Brune, W. (2020). Repression of viral gene expression and replication by the unfolded protein response effector XBP1U. *ELife*, ***9***, 1–22. https://doi.org/10.7554/eLife.51804

Ho, D. V., & Chan, J. Y. (2015). Induction of Herpud1 expression by ER stress is regulated by Nrf1. *FEBS Letters*, ***589***(5), 615–620. https://doi.org/10.1016/j.febslet.2015.01.026

Hwang, J., & Qi, L. (2018). Quality control in the endoplasmic reticulum: crosstalk between ERAD and UPR pathways. *Trends in Biochemical Sciences*, ***43***(8), 593–605. https://doi.org/10.1016/j.tibs.2018.06.005

Ibrahim, I. M., Abdelmalek, D. H., & El, A. A. (2019). GRP78: A cell's response to stress. *Life Sciences* ***226***. 156-163.

Jennings, P., Limonciel, A., Felice, L., & Leonard, M. O. (2013). An overview of transcriptional regulation in response to toxicological insult, ***87,*** 49–72. https://doi.org/10.1007/s00204-012-0919-y

Juszkiewicz, S., & Hegde, R. S. (2018). Quality Control of Orphaned Proteins. *Molecular Cell*, ***71***(3), 443–457. https://doi.org/10.1016/j.molcel.2018.07.001

Kim, H. M., Han, J. W., & Chan, J. Y. (2016). Nuclear Factor Erythroid-2 Like 1 (NFE2L1): Structure, function and regulation. *Gene*, ***584***(1), 17–25. https://doi.org/10.1016/j.gene.2016.03.002

Kim, S., Sideris, D. P., Sevier, C. S., & Kaiser, C. A. (2012). Balanced Ero1 activation and inactivation establishes ER redox homeostasis. *Journal of Cell Biology*, ***196***(6), 713–725. https://doi.org/10.1083/jcb.201110090

Kobayashi, A., & Waku, T. (2020). New addiction to the NRF2-related factor NRF3 in cancer cells: Ubiquitin-independent proteolysis through the 20S proteasome. *Cancer Science*, ***111***(1), 6–14. https://doi.org/10.1111/cas.14244

Koizumi, S., Irie, T., Hirayama, S., Sakurai, Y., Yashiroda, H., Naguro, I., … Murata, S. (2016). The aspartyl protease DDI2 activates Nrf1 to compensate for proteasome dysfunction. *ELife*, ***5***(AUGUST), 1–10. https://doi.org/10.7554/eLife.18357

Kostova, Z., & Wolf, D. H. (2003). For whom the bell tolls: Protein quality control of the endoplasmic reticulum and the ubiquitin-proteasome connection. *EMBO Journal*, ***22***(10), 2309–2317. https://doi.org/10.1093/emboj/cdg227

Lakkaraju, A. K. K., Mary, C., Scherrer, A., Johnson, A. E., & Strub, K. (2008). SRP maintains nascent chains translocation-competent by slowing translation rates to match limiting numbers of targeting sites. *Cell*, ***133***(3), 440–451. Retrieved from https://www.ncbi.nlm.nih.gov/pmc/articles/PMC3624763/pdf/nihms412728.pdf

Lee, A. H., Iwakoshi, N. N., Anderson, K. C., & Glimcher, L. H. (2003). Proteasome inhibitors disrupt the unfolded protein response in myeloma cells. *Proceedings of the National Academy of Sciences of the United States of America*, ***100***(17), 9946–9951. https://doi.org/10.1073/pnas.1334037100

Lee, J., & Ozcan, U. (2014). Unfolded protein response signaling and metabolic diseases. *Journal of Biological Chemistry*, ***289***(3), 1203–1211. https://doi.org/10.1074/jbc.R113.534743

Li, F., Gao, B., Dong, H., Shi, J., & Fang, D. (2015). Icariin induces Synoviolin expression through NFE2L1 to protect neurons from ER stress-induced apoptosis. *PLoS ONE*, ***10***(3), 21–27. https://doi.org/10.1371/journal.pone.0119955

Li, Y., & Camacho, P. (2004). Ca2+-dependent redox modulation of SERCA 2b by ERp57. *Journal of Cell Biology*, ***164***(1), 35–46. https://doi.org/10.1083/jcb.200307010

Liu, J., Schuff-Werner, P., & Steiner, M. (2004). Double transfection improves small interfering RNA-induced thrombin receptor (PAR-1) gene silencing in du 145 prostate cancer cells. FEBS Letters, **577**(1–2), 175–180. https://doi.org/10.1016/j.febslet.2004.09.079

Lynes, E. M., Raturi, A., Shenkman, M., Sandoval, C. O., Yap, M. C., Wu, J., … Simmen, T. (2013). Palmitoylation is the switch that assigns calnexin to quality control or ER Ca2+ signaling. *Journal of Cell Science*, ***126***(17), 3893–3903. https://doi.org/10.1242/jcs.125856

Määttänen, P., Gehring, K., Bergeron, J. J. M., & Thomas, D. Y. (2010). Protein quality control in the ER: The recognition of misfolded proteins. *Seminars in Cell and Developmental Biology*, ***21***(5), 500–511. https://doi.org/10.1016/j.semcdb.2010.03.006

Marcus, N., Shaffer, D., Farrar, P., & Green, M. (1996). Tissue distribution of three members of the murine protein disulfide isomerase (PDI) family. *Biochimica et Biophysica Acta - Gene Structure and Expression*, ***1309***(3), 253–260. https://doi.org/10.1016/S0167-4781(96)00133-9

McCaffrey, K., & Braakman, I. (2016). Protein quality control at the endoplasmic reticulum. *Essays in Biochemistry*, ***60***(2), 227–235. https://doi.org/10.1042/EBC20160003

Missiroli, S., Danese, A., Iannitti, T., Patergnani, S., Perrone, M., Previati, M., … Pinton, P. (2017). Endoplasmic reticulum-mitochondria Ca2 + crosstalk in the control of the tumor cell fate. *Biochimica et Biophysica Acta - Molecular Cell Research*, ***1864***(6), 858–864. https://doi.org/10.1016/j.bbamcr.2016.12.024

Moenner, M., Pluquet, O., Bouchecareilh, M., & Chevet, E. (2007). Integrated endoplasmic reticulum stress responses in cancer. *Cancer Research*, ***67***(22), 10631–10634. https://doi.org/10.1158/0008-5472.CAN-07-1705

Moon, H. W., Han, H. G., & Jeon, Y. J. (2018). Protein quality control in the endoplasmic reticulum and cancer. *International Journal of Molecular Sciences*, ***19***(10). https://doi.org/10.3390/ijms19103020

Myhill N., Lynes E. M., Nanji J. A., Fei H., Cooper T. J., G. T., & and Simmen T.. (2008). The subcellular distribution of calnexin is mediated by PACS-2. *Molecular Biology of the Cell*, ***19***(July), 2777–2788. https://doi.org/10.1091/mbc.E07dobson

Nakamura, K., Zuppini, A., Arnaudeau, S., Lynch, J., Ahsan, I., Krause, R., … Michalak, M. (2001). Functional specialization of calreticulin domains. *Journal of Cell Biology*, ***154(***5), 961–972. https://doi.org/10.1083/jcb.200102073

Nougarède, A., Tesnière, C., Ylanko, J., Rimokh, R., Gillet, G., & Andrews, D. W. (2018). Improved IRE1 and PERK pathway sensors for multiplex endoplasmic reticulum stress assay reveal stress response to nuclear dyes used for image segmentation. *Assay and Drug Development Technologies*, ***16***(6), 350–360. https://doi.org/10.1089/adt.2018.862

Okazaki, A., Jo, J. I., & Tabata, Y. (2007). A reverse transfection technology to genetically engineer adult stem cells. Tissue Engineering, ***13***(2), 245–251. https://doi.org/10.1089/ten.2006.0185

Olivari, S., Galli, C., Alanen, H., Ruddock, L., & Molinari, M. (2005). A novel stress-induced EDEM variant regulating endoplasmic reticulum-associated glycoprotein degradation. *Journal of Biological Chemistry*, ***280***(4), 2424–2428. https://doi.org/10.1074/jbc.C400534200

Phillips, B. P., Gomez-Navarro, N., & Miller, E. A. (2020). Protein quality control in the endoplasmic reticulum. *Current Opinion in Cell Biology*, ***65***, 96–102. https://doi.org/10.1016/j.ceb.2020.04.002

Pobre, K. F. R., Poet, G. J., & Hendershot, L. M. (2019). The endoplasmic reticulum (ER) chaperone BiP is a master regulator of ER functions: Getting by with a little help from ERdj friends. *Journal of Biological Chemistry*, ***294***(6), 2098–2108. https://doi.org/10.1074/jbc.REV118.002804

Remondelli, P., & Renna, M. (2017). The endoplasmic reticulum unfolded protein response in neurodegenerative disorders and its potential therapeutic significance. *Frontiers in Molecular Neuroscience*, ***10***(June), 1–16. https://doi.org/10.3389/fnmol.2017.00187

Robledinos-Antón, N., Fernández-Ginés, R., Manda, G., & Cuadrado, A. (2019). Activators and inhibitors of NRF2: a review of their potential for clinical development. *Oxidative Medicine and Cellular Longevity*, *2019*. https://doi.org/10.1155/2019/9372182

Rousseau, F., Serrano, L., & Schymkowitz, J. W. H. (2006). How evolutionary pressure against protein aggregation shaped chaperone specificity. *Journal of Molecular Biology*, ***355***(5), 1037–1047. https://doi.org/10.1016/j.jmb.2005.11.035

Sado, M., Yamasaki, Y., Iwanaga, T., Onaka, Y., Ibuki, T., Nishihara, S., … Watanabe, T. K. (2009). Protective effect against Parkinson's disease-related insults through the activation of XBP1. *Brain Research*, ***1257,*** 16–24. https://doi.org/10.1016/j.brainres.2008.11.104

Scheper, W., & Hoozemans, J. J. M. (2015). The unfolded protein response in neurodegenerative diseases: a neuropathological perspective. *Acta Neuropathologica*, ***130***(3), 315–331. https://doi.org/10.1007/s00401-015-1462-8

Schmidlin, C. J., Dodson, M. B., Madhavan, L., & Zhang, D. D. (2019). Redox regulation by NRF2 in aging and disease. *Free Radical Biology and Medicine*, ***134***(December 2018), 702–707. https://doi.org/10.1016/j.freeradbiomed.2019.01.016

Schrag, J. D., Procopio, D. O., Cygler, M., Thomas, D. Y., & Bergeron, J. J. M. (2003). Lectin control of protein folding and sorting in the secretory pathway. *Trends in Biochemical Sciences*, ***28***(1), 49–57. https://doi.org/10.1016/S0968-0004(02)00004-X

Sevier, C. S., & Kaiser, C. A. (2008). Ero1 and redox homeostasis in the endoplasmic reticulum. *Biochimica et Biophysica Acta - Molecular Cell Research*, ***1783***(4), 549–556. https://doi.org/10.1016/j.bbamcr.2007.12.011

Sevier, C. S., Qu, H., Heldman, N., Gross, E., Fass, D., & Kaiser, C. A. (2007). Modulation of cellular disulfide-bond formation and the ER redox environment by feedback regulation of Ero1. *Cell*, ***129***(2), 333–344. https://doi.org/10.1016/j.cell.2007.02.039

Sha, Z., & Goldberg, A. L. (2014). Proteasome-mediated processing of Nrf1 is essential for coordinate induction of all proteasome subunits and p97. *Current Biology*, ***24***(14), 1573–1583. https://doi.org/10.1016/j.cub.2014.06.004

Shan, Y., Napoli, E., & Cortopassi, G. (2007). Mitochondrial frataxin interacts with ISD11 of the NFS1/ISCU complex and multiple mitochondrial chaperones. *Human Molecular Genetics*, ***16***(8), 929–941. https://doi.org/10.1093/hmg/ddm038

Sherman, D. J., & Li, J. (2020). Proteasome inhibitors: Harnessing proteostasis to combat disease. *Molecules*, ***25***(3), 1–30. https://doi.org/10.3390/molecules25030671

Steffen, J., Seeger, M., Koch, A., & Krüger, E. (2010). Proteasomal degradation is transcriptionally controlled by TCF11 via an ERAD-dependent feedback loop. *Molecular Cell*, ***40***(1), 147–158. https://doi.org/10.1016/j.molcel.2010.09.012

Strub, K., Moss, J., & Walter, P. (1991). Binding sites of the 9- and 14-kilodalton heterodimeric protein subunit of the signal recognition particle (SRP) are contained exclusively in the Alu domain of SRP RNA and contain a sequence motif that is conserved in evolution. *Molecular and Cellular Biology*, ***11***(8), 3949–3959. https://doi.org/10.1128/mcb.11.8.3949

Suda, N., Itoh, T., Nakato, R., Shirakawa, D., Bando, M., Katou, Y., … Tanaka, M. (2014). Dimeric combinations of MafB, cFos and cJun control the apoptosis-survival balance in limb morphogenesis. *Development (Cambridge)*, ***141***(14), 2885–2894. https://doi.org/10.1242/dev.099150

Sun, Z., & Brodsky, J. L. (2019). Protein quality control in the secretory pathway. *Journal of Cell Biology*, ***218***(10), 3171–3187. https://doi.org/10.1083/jcb.201906047

Sykiotis, G. P., & Bohmann, D. (2010). Stress-activated cap'n'collar transcription factors in aging and human disease. *Science Signaling*, ***3***(112). https://doi.org/10.1126/scisignal.3112re3

Tavender, T. J., & Bulleid, N. J. (2010). Peroxiredoxin IV protects cells from oxidative stress by removing H 2O2 produced during disulphide formation. Journal of Cell Science, ***123***(15), 2672–2679. https://doi.org/10.1242/jcs.067843

Tirosh, B., Iwakoshi, N. N., Glimcher, L. H., & Ploegh, H. L. (2006). Rapid turnover of unspliced Xbp-1 as a factor that modulates the unfolded protein response. *Journal of Biological Chemistry*, ***281***(9), 5852–5860. https://doi.org/10.1074/jbc.M509061200

Tomlin, F. M., Gerling-Driessen, U. I. M., Liu, Y. C., Flynn, R. A., Vangala, J. R., Lentz, C. S., … Bertozzi, C. R. (2017). Inhibition of NGLY1 inactivates the transcription factor Nrf1 and potentiates proteasome inhibitor cytotoxicity. *ACS Central Science*, ***3***(11), 1143–1155. https://doi.org/10.1021/acscentsci.7b00224

Tsuchiya, Y., Morita, T., Kim, M., Iemura, S. -i., Natsume, T., Yamamoto, M., & Kobayashi, A. (2011). Dual Regulation of the Transcriptional Activity of Nrf1 by -TrCP- and Hrd1-Dependent Degradation Mechanisms. *Molecular and Cellular Biology*, ***31***(22), 4500–4512. https://doi.org/10.1128/mcb.05663-11

Tsuru, A., Imai, Y., Saito, M., & Kohno, K. (2016). Novel mechanism of enhancing IRE1α-XBP1 signalling via the PERK-ATF4 pathway. *Scientific Reports*, ***6***, 1–8. https://doi.org/10.1038/srep24217

Uhrigshardt, H., Singh, A., Kovtunovych, G., Ghosh, M., & Rouault, T. A. (2010). Characterization of the human HSC20, an unusual DnaJ type III protein, involved in iron-

sulfur cluster biogenesis. *Human Molecular Genetics*, ***19***(19), 3816–3834. https://doi.org/10.1093/hmg/ddq301

Valdés, P., Mercado, G., Vidal, R. L., Molina, C., Parsons, G., Court, F. A., … Hetz, C. (2014). Control of dopaminergic neuron survival by the unfolded protein response transcription factor XBP1. *Proceedings of the National Academy of Sciences of the United States of America*, ***111***(18), 6804–6809. https://doi.org/10.1073/pnas.1321845111

Verkhratsky, A., & Toescu, E. C. (2003). Endoplasmic reticulum Ca^{2+} homeostasis and neuronal death. *Journal of Cellular and Molecular Medicine*, ***7***(4), 351–361. https://doi.org/10.1111/j.1582-4934.2003.tb00238.x

Voisine, C., Pedersen, J. S., & Morimoto, R. I. (2010). Chaperone networks: Tipping the balance in protein folding diseases. *Neurobiology of Disease*, ***40***(1), 12–20. https://doi.org/10.1016/j.nbd.2010.05.007

Waku, T., Katayama, H., Hiraoka, M., Hatanaka, A., Nakamura, N., Tanaka, Y., … Kobayashi, A. (2020). NFE2L1 and NFE2L3 Complementarily maintain basal proteasome activity in cancer cells through CPEB3-mediated translational repression. *Molecular and Cellular Biology*, ***40***(14). https://doi.org/10.1128/mcb.00010-20

Wang, W., & Chan, J. Y. (2006). Nrf1 is targeted to the endoplasmic reticulum membrane by an N-terminal transmembrane domain: Inhibition of nuclear translocation and transacting function. *Journal of Biological Chemistry*, *281*(28), 19676–19687. https://doi.org/10.1074/jbc.M602802200

Wang, J., Lee, J., Liem, D.,Ping, P. (2017) HSPA5 gene encoding Hsp70 chaperone Bip in the endoplasmic reticulum. *Gene*, ***294***, 14-23.

Wang, F.-M., & Ouyang, H.-J. (2011). Regulation of unfolded protein response modulator XBP1s by acetylation and deacetylation. *Biochem J.*, ***433***(1), 245–252. https://doi.org/10.1042/BJ20101293.Regulation

Wang, Y., Zhang, Y., Yi, P., Dong, W., Nalin, A. P., Zhang, J., … Yu, J. (2019). The IL-15–AKT–XBP1s signaling pathway contributes to effector functions and survival in human NK cells. *Nature Immunology*, ***20***(1), 10–17. https://doi.org/10.1038/s41590-018-0265-1

Wu, S., Du, R., Gao, C., Kang, J., Wen, J., & Sun, T. (2018). The role of XBP1s in the metastasis and prognosis of hepatocellular carcinoma. *Biochemical and Biophysical Research Communications*, ***500***(3), 530–537. https://doi.org/10.1016/j.bbrc.2018.04.033

Xiang, Y., Wang, M., Hu, S., Qiu, L., Yang, F., Zhang, Z., … Zhang, Y. (2018). Mechanisms controlling the multistage post-translational processing of endogenous Nrf1α/TCF11 proteins to yield distinct isoforms within the coupled positive and negative feedback circuits. *Toxicology and Applied Pharmacology*, ***360***(September), 212–235. https://doi.org/10.1016/j.taap.2018.09.036

Xie, J., Tao, Z. H., Zhao, J., Li, T., Wu, Z. H., Zhang, J. F., … Hu, X. C. (2016). Glucose regulated protein 78 (GRP78) inhibits apoptosis and attentinutes chemosensitivity of gemcitabine in breast cancer cell via AKT/mitochondrial apoptotic pathway. *Biochemical and Biophysical Research Communications*, ***474***(3), 612–619. https://doi.org/10.1016/j.bbrc.2016.03.002

Yanagitani, K., Kimata, Y., Kadokura, H., & Kohno, K. (2011). Membrane targeting and cytoplasmic splicing of XBP1u mRNA. *Science*, ***331***(February), 586–590.

Yoo, J., Mashalidis, E. H., Kuk, A. C. Y., Yamamoto, K., Kaeser, B., Ichikawa, S., & Lee, S. Y. (2018). GlcNAc-1-P-transferase-tunicamycin complex structure reveals basis for inhibition of N-glycosylation. *Nature Structural and Molecular Biology*, ***25***(3), 217–224. https://doi.org/10.1038/s41594-018-0031-y

Yoshida, H., Matsui, T., Yamamoto, A., Okada, T., & Mori, K. (2001). XBP1 mRNA is induced by ATF6 and spliced by IRE1 in response to ER stress to produce a highly active transcription factor. *Cell*, ***107***(7), 881–891. https://doi.org/10.1016/S0092-8674(01)00611-0

Yoshida, H., Oku, M., Suzuki, M., & Mori, K. (2006). pXBP1(U) encoded in XBP1 pre-mRNA negatively regulates unfolded protein response activator pXBP1(S) in mammalian ER stress response. *Journal of Cell Biology*, ***172***(4), 565–575. https://doi.org/10.1083/jcb.200508145

Yoshida, H., Uemura, A., & Mori, K. (2009). pXBP1(U), a negative regulator of the unfolded protein response activator pXBP1(S), targets ATF6 but not ATF4 in proteasome-mediated degradation. *Cell Structure and Function*, ***34***(1), 1–10. https://doi.org/10.1247/csf.06028

Yuan, J., Wang, H., Xiang, Y., Hu, S., Li, S., Wang, M., … Zhang, Y. (2018). Nrf1D is the first candidate secretory transcription factor in the blood plasma, its precursor existing as a unique redox-sensitive transmembrane CNC-bZIP protein in hemopoietic and somatic tissues. *International Journal of Molecular Sciences*, ***19***(10). https://doi.org/10.3390/ijms19102940

Zhang, Y., & Hayes, J. D. (2013). The membrane-topogenic vectorial behaviour of Nrf1 controls its post-translational modification and transactivation activity. *Scientific Reports*, ***3***, 1–16. https://doi.org/10.1038/srep02006

Zhang, Y., Li, S., Xiang, Y., Qiu, L., Zhao, H., & Hayes, J. D. (2015). The selective post-translational processing of transcription factor Nrf1 yields distinct isoforms that dictate its ability to differentially regulate gene expression. *Scientific Reports*, ***5***(174), 1–30. https://doi.org/10.1038/srep12983

Zhang, Y., Lucocq, J. M., & Hayes, J. D. (2009). The Nrf1 CNC/bZIP protein is a nuclear envelope-bound transcription factor that is activated by t-butyl hydroquinone but not by endoplasmic reticulum stressors. *Biochemical Journal*, ***418***(2), 293–310. https://doi.org/10.1042/BJ20081575

Zhang, Y., & Manning, B. D. (2015). mTORC1 signaling activates NRF1 to increase cellular proteasome levels. *Cell Cycle*, ***14***(13), 2011–2017. https://doi.org/10.1080/15384101.2015.1044188

Zhang, Z., Zhang, L., Zhou, L., Lei, Y., Zhang, Y., & Huang, C. (2019). Redox signaling and unfolded protein response coordinate cell fate decisions under ER stress. *Redox Biology*, ***25***(September 2018), 101047. https://doi.org/10.1016/j.redox.2018.11.005

Zhu, Y. P., Zheng, Z., Hu, S., Ru, X., Fan, Z., Qiu, L., & Zhang, Y. (2020). Unification of opposites between two antioxidant transcription factors nrf1 and nrf2 in mediating distinct cellular responses to the endoplasmic reticulum stressor tunicamycin. *Antioxidants*, ***9***(1). https://doi.org/10.3390/antiox9010004

Appendix A: NFE2L1 Overexpression and Knockdown RT-qPCR Validation

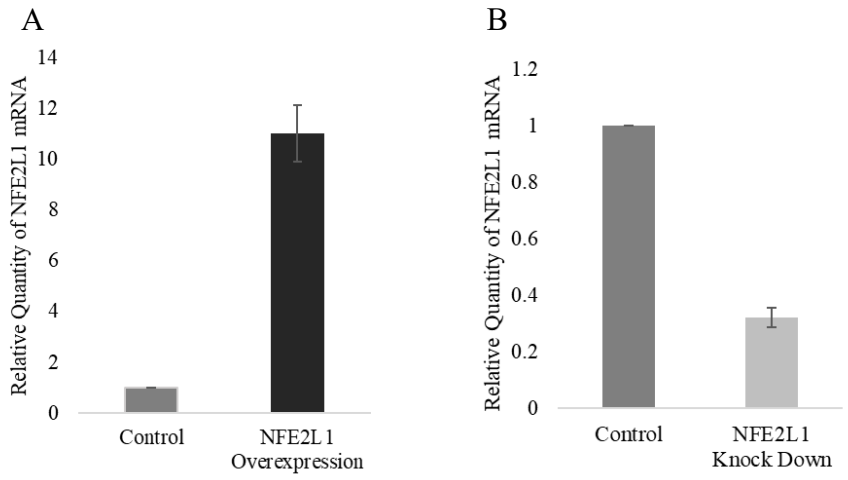

Figure 11: NFE2L1 Overexpression and Knockdown RT-qPCR Validation. HCT116 were either double-transfected with NFE2L1-targeting dsRNAi for knock down (A) using the Oligofectamine reagent, or reverse-tranfected once with a plasmid expressing NFE2L1 for overexpression (B). N=6.

Appendix B: Sample Plots – qPCR and Flow Cytometry

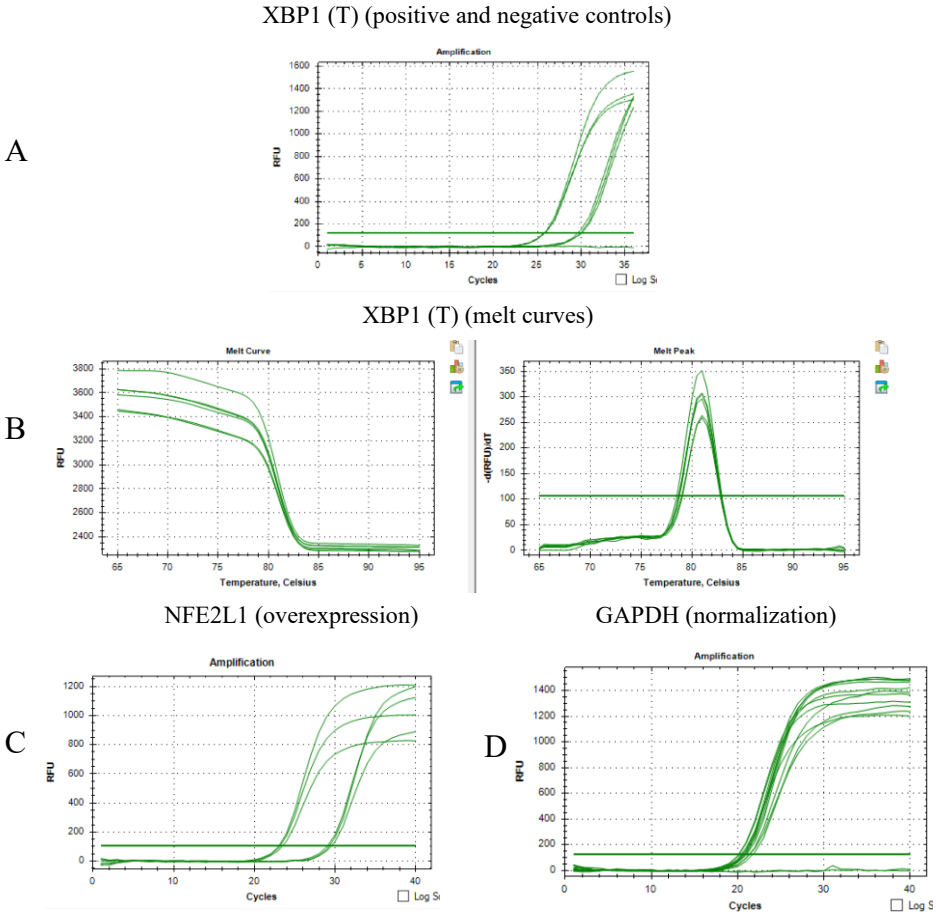

Figure 12: Sample qPCR plots; XBP1(T) controls (A), XBP1(T) melt curve (B), NFE2L1 overexpression (C) and GAPDH normalization plot (D). (A) Amplicon on left is the positive control (control, treated) and right amplicon is negative control (control, untreated). (A/D) Line along the bottom represents the no template control sample (substituted cDNA with deionized water). (C) Amplicon on left is overexpressing NFE2L1, amplicon on the right is the control transfected with the empty PUC19 vector. (D) All samples normalized to control, untreated

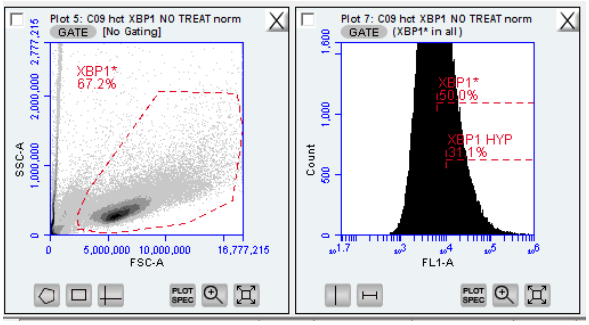

Figure 13: Sample flow cytometry live cell gating (A) and XBP1(S) flow plot fluorescence analysis (B). This was done using the HCT116 cell line that expresses mNeonGreen-conjugated XBP1(S) under ER stress conditions. XBP1* refers to the reference fluorescence under control conditions; XBP1 HYP refers to XBP1(S) fluorescence when treated with 1% oxygen for 24 hours (which induces ER stress). Total events: 50 000.

Appendix C: mNeonGreen-Conjugated XBP1-Expressing HCT116 Cell Line Construct

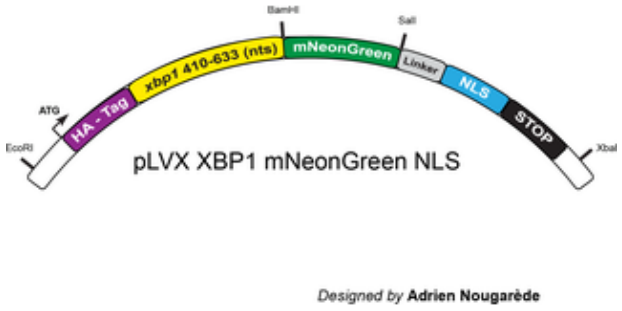

Figure 14: Construct for stably transfected HA-Tagged mNeonGreen-conjugated XBP1(S) in HCT116 cell line. Reporter used for fluorescence microscopy and flow cytometry. (Nougarède *et al*., 2018)